Highlights

- Local population and social group size estimates were smaller in the invasive range.
- Invasive range parakeets produced calls with simpler individual signatures.
- Urban calls had simpler frequency modulation patterns in the native and invasive ranges.
- Monk parakeets may use vocal learning for individual vocal recognition.

Individual vocal signatures show reduced complexity following invasion

Grace Smith-Vidaurre [a, b, c, d, *], Valeria Perez-Marrufo [a], Timothy F. Wright [a]

[a] *Department of Biology, New Mexico State University, Las Cruces, NM, U.S.A.*

[b] *Laboratory of Neurogenetics of Language, Rockefeller University, New York, NY, U.S.A.*

[c] *Rockefeller University Field Research Center, Millbrook, NY, U.S.A.*

[d] *Department of Biological Sciences, University of Cincinnati, Cincinnati, OH, U.S.A.*

Article history:

Received 14 September 2020

Initial acceptance 3 November 2020

Final acceptance 21 April 2021

Available online 19 July 2021

MS. number: A20-00691R

* Corresponding author.

E-mail address: gsvidaurre@gmail.com (G. Smith-Vidaurre).

Rockefeller University Field Research Center, Millbrook, NY, U.S.A.

The manner in which vocal learning is used for social recognition may be sensitive to the social environment. Biological invaders capable of vocal learning are useful for testing this possibility, as invasion alters population size. Some vocal learning species use frequency modulation patterns of acoustic signals for individual recognition. In such species, frequency modulation patterns should be more complex in larger social groups, reflecting greater selection for individual distinctiveness. We used numbers of nests and nest densities as proxies of local population sizes of native range monk parakeets, *Myiopsitta monachus*, in Uruguay and invasive range populations in the United States. Flock sizes were obtained to estimate maximum social group sizes per range. Supervised machine learning and frequency contours were employed to compare contact call structure between native and invasive range populations, and the effect of urban habitats on call structure was also assessed. Invasive range populations exhibited fewer nests, lower nest densities and smaller maximum flock sizes, which is consistent with a reduction in population size following invasion. Parakeets at invasive range sites also produced contact calls with simpler frequency modulation patterns. Beecher's statistic (HS) revealed reduced individual identity content and fewer possible unique individual signatures in invasive range calls. Simpler individual signatures are consistent with relaxed selection on the complexity of learned calls likely used for individual vocal recognition in the smaller local populations that we identified post-invasion. Frequency modulation patterns were simpler in urban habitats in both ranges, indicating that urban habitats could also alter the social environment and in turn influence the complexity of learned individual signatures. These findings contribute to a growing literature on the use of vocal learning for individual recognition and indicate that vocal learning can be used to produce individual vocal signatures in a manner sensitive to local population size.

Keywords:
bioacoustics
biological invader
contact call
frequency modulation

individual recognition

individual signature

monk parakeet

Myiopsitta monachus

random forests

vocal learning

One way in which vocal learning can be used in communication systems is to signal group identity for social recognition (Janik & Slater, 2000; Nowicki & Searcy, 2014; Sewall, Young, & Wright, 2016). Patterns of acoustic convergence within social groups consistent with vocal learning being used for group recognition have been identified in cetaceans, bats, songbirds and parrots (Sewall et al., 2016). Vocal learning may also be used to create individually distinctive acoustic signals, often termed 'individual signatures', as found in many of the same taxonomic groups (Berg, Delgado, Okawa, Beissinger, & Bradbury, 2011; Berg, Delgado, Cortopassi, Beissinger, & Bradbury, 2012; Fripp et al., 2005; Janik, Sayigh, & Wells, 2006). The manner in which different taxa use vocal learning to recognize group members could be sensitive to population size and social dynamics.

Larger social groups contain more individuals among which potential receivers must discriminate, leading to increased uncertainty about signallers' identities and increased selection on signallers to produce distinctive individual signatures (Pollard & Blumstein, 2011; Tibbetts & Dale, 2007). In species that use vocal learning for individual vocal recognition, selection to produce individually distinctive signals should manifest itself in the acoustic structure of learned calls. For instance, learning can be used to produce individually distinctive frequency modulation patterns in acoustic signals (Berg et al., 2011; Fripp et al., 2005; Janik et al., 2006). In such systems, frequency modulation patterns in learned signals should be more complex in larger social groups and simpler in smaller social groups, leading to fewer possible unique individual signatures in the acoustic space of smaller social groups (Beecher, 1989). Biological invaders offer useful models for addressing this hypothesis, as invasive populations often exhibit reduced population sizes compared to the native range shortly after introduction (Duncan, Blackburn, & Sol, 2003; Estoup et al., 2016) and could either remain small in the absence of population growth or, in some cases, grow to reach sizes comparable to populations in the native range.

We asked whether the way in which vocal learning is used for social recognition is resilient or sensitive to changes in population size by evaluating contact calls of an invasive parrot. Monk parakeets, *Myiopsitta monachus*, are native to South America, may use vocal learning for individual recognition (Smith-

Vidaurre, Araya-Salas, & Wright, 2020), display complex fission–fusion social dynamics (Hobson, Avery, & Wright, 2014) and have established invasive populations across the world through the pet trade (Russello, Avery, & Wright, 2008). One of the earliest established populations of invasive range monk parakeets in the Northern Hemisphere was documented in 1969 in Florida in the United States of America (U.S.) (Edelaar et al., 2015), and invasive range populations were established in seven different states in the U.S. by the early 1970s (Van Bael & Pruett-Jones, 1996). Populations in Connecticut, U.S., are thought to have been founded by a first introduction in 1973, with a possible second introduction in 1985 (Edelaar et al., 2015). Monk parakeets therefore provide the opportunity to evaluate patterns of variation in learned acoustic signals following multiple recent invasions.

In this study, native range monk parakeets were recorded in Uruguay in 2017, and invasive range populations were recorded in the U.S. in sampling intervals that spanned 15 years. We obtained estimates of total nests and nest densities at nesting sites as proxies of local population sizes and estimates of maximum flock sizes as a proxy for maximum social group sizes in each range. We predicted that in the absence of significant population growth post-invasion, invasive range populations would be smaller than native range populations at the time of sampling and that frequency modulation patterns in invasive range contact calls would be simpler compared to the native range. We also asked whether call structure changed over time in the invasive range. Invasive range populations that grew to large sizes over time could experience greater selection for more distinctive individual signatures, confounding direct comparisons between ranges. However, if invasive range populations did not grow to native range population sizes after the initial stages of invasion, as suggested by previous work documenting slower population growth rates or population declines in the last two decades (Pruett-Jones & Tarvin, 1998; Pruett-Jones et al., 2012), then we expected simpler frequency modulation patterns in invasive range calls to persist over our sampling intervals.

Finally, we assessed the effect of habitat differences on contact call acoustic structure, as our comparison between ranges included a partial confound of habitat. Native range parakeets were largely recorded in nonurban habitats, although some calls were recorded in urban areas. Most invasive range populations in the

U.S. are limited to urban centres (Davis, Malas, & Minor, 2014), which are characterized by anthropogenic noise that can mask avian acoustic signals (Halfwerk & Slabbekoorn, 2009, 2014). However, we did not expect urban habitats to exert a stronger influence on frequency modulation patterns than monk parakeets' social environments, given this species' nest-building behaviour. Monk parakeets build nests in which they roost year-round (Burgio et al., 2020; Eberhard, 1998), and most social interactions revolve around nesting sites (Burgio et al., 2020; Sol, Santos, Feria, Clavell, & Feria, 1997), which ties the majority of parakeets' social interactions and acoustic signalling to green spaces that should exhibit less anthropogenic noise. As urban green spaces are often smaller and geographically isolated compared to nonurban habitats (Goddard, Dougill, & Benton, 2010), urban parakeets also should experience fewer opportunities for social interactions, placing an upper limit on social group sizes in urban habitats. We anticipated that if social environments were altered in urban habitats, then frequency modulation patterns would be simpler in urban calls compared to nonurban calls. If urban parakeets were responding to masking by anthropogenic noise, then we expected that urban calls would exhibit increased pitch compared to nonurban calls, as documented in acoustic signals of other avian species (Halfwerk et al., 2011; Halfwerk & Slabbekoorn, 2009, 2014; Hu & Cardoso, 2010).

METHODS

Obtaining Total Nests and Nest Densities as Proxies of Local Population Size per Range

Monk parakeets build communal and colonial nests using sticks collected from nearby vegetation (Burgio et al., 2020; Eberhard, 1998). These stick nests can be single or multichambered structures, with one or more individuals living in any single nest (Burgio et al., 2020; Eberhard, 1998). Nests are often built in close proximity, and parakeets spend most of their time at nesting sites throughout the year (Burgio et al., 2020; Eberhard, 1998). As monk parakeets have been considered agricultural pests in their native range since the early 1800s (Russello et al., 2008) and can cause fires by nesting on electrical transformers in their invasive range,

nests are often removed in attempts to control populations (Avery, Tillman, Keacher, Arnett, & Lundy, 2012). However, nests are often rebuilt in the same or nearby structures (see Appendix, Pest control and proxies of local population size) (Burgio et al., 2020; G. Smith-Vidaurre, personal observation). We used the estimated number of nests and nest densities at nesting sites as proxies of local population sizes in each range, following previous work that also relied on nests to estimate population density of invasive range parakeets in Spain (Sol et al., 1997).

We estimated the numbers of nests at 20 native range nesting sites in 2017 and at 17 invasive range nesting sites in 2011, 2018 and 2019 by counting the nests visible at each site (Appendix, Table A2). Nests were considered independent structures when they were visibly separate, even when built in the same tree or artificial structure. Single and multichambered nests were counted as a single structure. Nests were detected via visual surveys of trees and artificial structures, as well as by observing parakeets' activity. Although the detectability of nests was high, our access to nesting sites was sometimes restricted by access to private properties in both ranges. Therefore, the numbers of nests reported here should be considered estimates because other nests in the vicinity may have been missed. We did not infer the number of individuals present at a given nesting site, because it was not always possible to evaluate whether nests were active and because we could not always count the number of nest chambers or the number of individuals residing in each chamber.

Nesting site areas were obtained for 16 and 10 sites in the native and invasive ranges, respectively, to assess whether nesting site areas and nest densities differed between ranges. Polygons for nesting sites were traced in Google My Maps when site boundaries were clearly visible in the 2020 imagery employed by Google Maps, and the total area of each nesting site polygon was calculated in R (R Core Team, 2018) to obtain an estimate of the geographical area encompassed by each nesting site in hectares. We relied on field observations to draw polygons that represented the minimum area encompassed by nests observed at each site. The nest density at each site was estimated by dividing the number of nests observed by the nesting site area. The median and interquartile range (IQR) of each variable was obtained per range. Two-sided Mann–Whitney–Wilcoxon tests were employed to assess whether these three nest variables differed significantly between ranges, as data

were not normally distributed. To meet the assumption of independent samples, we retained a single observation per nesting site when nesting sites were evaluated in more than one year.

Obtaining Maximum Flock Size Estimates in Each Range

The complex social environment of monk parakeets is characterized by social interactions in different contexts, including interactions at nesting sites and during foraging events (Hobson et al., 2014). We obtained eight and six observations of maximum flock sizes for the native and invasive ranges, respectively, which are representative of the largest social group sizes monk parakeets are likely to experience across social contexts (Hobson et al., 2014). The largest flock sizes observed per range were collected from field notebooks documenting native range fieldwork in Uruguay in 2017 and invasive range fieldwork in the United States in 2011 and 2019. Flocks observed of 100 to several hundred birds were set to a maximum estimate of 100, as exact counts had not been obtained. Parakeet flock sizes were observed while birds were foraging, flying and staging. We obtained the medians and interquartile ranges of maximum flock sizes observed during fieldwork in both ranges. Two-sided Mann–Whitney–Wilcoxon tests were used to determine whether maximum estimated flock sizes differed significantly between ranges. We retained a single observation per location that was repeatedly sampled in the same or different years to meet the assumption of independent samples.

Spatiotemporal Sampling of Native and Invasive Range Monk Parakeet Contact Calls

Native range contact calls were recorded in 2017 at nesting sites in Uruguay, as previously described (Smith-Vidaurre et al., 2020). Invasive range contact calls were recorded at nesting sites as well, hereafter referred to as ‘sites’, across five states in the U.S. over different years. For invasive range calls, we obtained previously published calls recorded in 2004 in Connecticut, Florida, Louisiana and Texas from authors of previous work (Buhrman-Deever, Rappaport, & Bradbury, 2007). We recorded calls ourselves in Texas and

Louisiana in 2011, in Arizona in 2018 and in Texas in 2019. All native range calls were previously published (Smith-Vidaurre et al., 2020), as were all invasive range calls recorded in 2004 (Buhrman-Deever et al., 2007). Invasive range calls recorded in 2011, 2018 and 2019 were not previously published.

Four of the native range sites at which we recorded were green spaces located within the city of Montevideo and were considered urban sites. Most invasive range sites were green spaces inside or near city centres in the U.S., and for the purposes of this study, we considered all invasive range sites to be urban sites. Nonurban sites in the native range were represented by clusters of nests located in or near small towns, as well as landscapes altered by agricultural activity (cattle grazing, dairies, seasonal crops), which we considered 'agro-interface' habitats (Appendix, Validating the Effect of Urban and Agro-interface Habitats between Ranges).

Contact Call Recording and Preprocessing

We performed recording sessions with Marantz PMD661 MKII and PMD660 solid-state recorders, Sennheiser ME67 long shotgun microphones and digitized the resulting audio files at 44 100 Hz sampling rate and 16-bit depth. Invasive range 2004 sessions employed Marantz PMD670 or PMD690 recorders with Sennheiser ME67/K6 shotgun microphones, and recordings were digitized at 48 000 Hz and 16 bits (Buhrman-Deever et al., 2007). Contact calls were generally obtained from parakeets that produced a single call while flying to or from nests. Invasive range calls were manually selected from recordings using Raven v.1.4 (Cornell Lab of Ornithology Bioacoustics Research Program, 2014) and preprocessed with the warbleR package in R to retain high-quality calls following procedures previously used for native range calls (Smith-Vidaurre et al., 2020).

For the purposes of this study, we used two data sets of calls. The first data set was composed of a single call per each unique individual recorded at each nesting site (hereafter referred to as 'sites') that provided broad geographical resolution of contact call variation in each range (Appendix, Tables A3, A4). This data set contained 1367 total calls recorded at 63 sites between the two ranges (37 native range and 26 invasive range

sites), which included sites sampled over multiple time points in the invasive range. The native range was represented by 610 calls, and the invasive range by 757 calls. Eleven invasive range sites were recorded in 2004, eight sites were recorded in 2011, one site was recorded in 2018 and six sites were recorded in 2019. Native range sites were represented by a median of 15 calls (range 5–53) per site, and invasive range sites were represented by a median of 15.5 calls (range 5–93) each. This data set was used to assess general differences in call structure between ranges as well as finer-scale variation in acoustic structure between ranges and over time in the invasive range.

The second data set contained calls of repeatedly sampled individuals, which provided sufficient sampling depth for assessing the occurrence of individual signatures in contact calls. Repeated contact calls per individual were obtained from bouts of vocalizations delivered over a brief period (often a few minutes), and we used calls that were recorded in a single day per individual (Smith-Vidaurre et al., 2020). This data set contained 229 total calls: 97 native range calls and 132 invasive range calls. These contact calls were obtained from 17 repeatedly sampled individuals: eight native range birds (3 marked, 5 unmarked) recorded from three sites in 2017 (Smith-Vidaurre et al., 2020) and nine unmarked invasive range birds recorded from seven sites in 2004, 2011 and 2019 (Appendix, Table A5) (Buhrman-Deever et al., 2007). Repeatedly sampled individuals were represented by a median of 10 calls (range 4–25) and 12 calls (range 5–28) per the native and invasive ranges, respectively. Calls of repeatedly sampled individuals were used to assess general differences in call structure between ranges and individual identity content present in individual signatures. All analyses reported below were performed in the R environment (R Core Team, 2018).

Assessing General Differences in Call Structure between Ranges

Overall differences in call structure between ranges were evaluated with supervised machine learning models that classified calls back to each range. Supervised machine learning provides a rigorous predictive modelling framework that can be a useful tool for behavioural questions (Valletta, Torney, Kings,

Thornton, & Madden, 2017). At the prediction step, the trained and validated model predicted the 'true' range of each call, given a diverse set of predictors that captured patterns of variation in contact call structure. Classification accuracy during prediction was used as an indication of general structural differences between ranges (e.g. low classification accuracy would indicate low structural differentiation between ranges).

Supervised stochastic gradient boosting (Friedman, 2001) and random forests models (Breiman, 2001) were built with 203 predictors, including 15 standard acoustic measurements and 188 acoustic features derived by multidimensional scaling (MDS) and principal components analysis (PCA) (see Appendix, Obtaining predictors for machine learning). Spectrum-based measurements were obtained using a Hanning window, spectrogram window length of 378 samples, window overlap of 90% (percentage of overlap between adjacent windows) for Fourier transformations and a band-pass filter of 0.5–9 kHz (Smith-Vidaurre et al., 2020). We used 1561 calls for predictive modelling and split these calls into training, validation and prediction data sets. Calls used for these analyses were pulled from both data sets described above. We visualized 548 calls (230 native, 318 invasive) that we used for predictions of the 'true' range per call in two-dimensional acoustic space by applying MDS to the proximity matrix of the final random forests model. A two-dimensional Gaussian kernel density estimator was applied to MDS coordinates to yield density contours per range in random forests acoustic space (see Appendix, Finer-scale assessment of structural change).

Assessing Frequency Modulation Patterns between Ranges and over Time

We subsampled 80 calls to evaluate frequency modulation patterns between ranges. We subsampled calls for this analysis because we relied on manual tracing to obtain customized frequency modulation measurements, and this would have been prohibitively time-consuming to perform for all calls. Ten sites were randomly selected per range, and four calls were randomly chosen per site (random sampling was performed without replacement). For temporal comparisons of frequency modulation patterns in the invasive range, we chose 15 sites from Austin, Texas and New Orleans, Louisiana that represented sampling over time.

We randomly selected five calls per site without replacement, yielding a total of 75 calls for these temporal comparisons in the invasive range, in addition to the 40 calls chosen for the native range (see Appendix, Comparisons of frequency modulation patterns and individual identity content). Calls chosen for comparisons of frequency modulation patterns between ranges and over time in the invasive range were selected from the large data set of broad geographical resolution in which each call represented a unique individual.

Three customized frequency modulation measurements were derived from frequency contours of the second harmonic per call: the number of peaks per call, the modulation rate (number of peaks divided by the duration of call) and the maximum slope of frequency modulation per call (largest negative slope between peaks and neighbouring troughs). To obtain frequency contours, we estimated fundamental frequencies at 100 time points per call and used these time series as a baseline for manually tracing the second harmonic, which was more clearly visible across a greater number of calls. Five points were dropped from the start and end of each frequency contour, as these points often fell underneath components of the graphical user interface employed for tailoring. Spline interpolation was performed across the remaining 90 points with smoothing, and smoothed contours were used to estimate frequency peaks and troughs and derive customized frequency modulation measurements per call (see Results, Fig. 3a).

The median and IQR of each of the three abovementioned customized frequency modulation measurements were obtained per range, as well as the 27 standard spectral acoustic measurements that were used to create features for supervised machine learning (Appendix, Table A7). These 27 acoustic measurements were duration, mean frequency, standard deviation of frequency, median frequency, first quartile frequency, third quartile frequency, frequency interquartile range, median time, first quartile time, third quartile time, time interquartile range, skew, kurtosis, spectral entropy, time entropy, entropy (product of spectral and time entropy), spectral flatness, the mean, minimum and maximum dominant frequency, dominant frequency range and slope, modulation index, start and end dominant frequency, peak frequency and mean peak frequency (Araya-Salas & Smith-Vidaurre, 2017). Fundamental frequency measurements were not used, as these were not accurate for monk parakeet calls. Each acoustic measurement was represented by a single value per call. The modulation

index represented the degree of modulation of the dominant frequency and was not equivalent to the modulation rate calculated with manually traced frequency contours (see Appendix, Calculating frequency modulation measurements).

The effect size of range on each of the 30 acoustic measurements (3 customized frequency modulation measurements and 27 standard spectral acoustic measurements) was calculated as Cliff's delta (Cliff, 1996). We obtained 95% confidence intervals (CIs) from 10 000 iterations of the bias-corrected and accelerated bootstrap method. Cliff's delta and the bootstrapping method were used because these statistics are less susceptible to non-normal data with heterogeneous variance (Chen & Chao-Ying, 2015; Hess & Kromrey, 2004) and because several of our acoustic measurements violated the assumptions of normality and equal variance underlying Cohen's *d* (Hess et al., 2004). Cliff's delta is bounded between -1 and 1, and reflects the degree of overlap between two distributions, such that a value of 0 indicates complete overlap of distributions and no significant difference between groups (Hess et al., 2004). For variables with a positive sign, negative values of Cliff's delta indicated larger values for a given acoustic measurement in the baseline group (the native range in this study), while positive values indicated the reverse (i.e. larger values of the given acoustic measurement for the invasive range). The opposite was true for variables with a negative sign (e.g. peak–trough slope). Effect sizes were statistically significant when 95% CIs did not include zero, and we considered effect sizes 'large' when absolute values were greater than or equal to 0.474 (Romano, Kromrey, Coraggio, Skowronek, & Devine, 2006). We assessed whether differences identified between ranges held over 15 years of sampling in the invasive range by visualizing the distributions of acoustic measurements for 115 calls.

Individual Identity Content and Frequency Contours of Calls

We used Beecher's statistic (HS) to quantify the amount of individual identity content in calls of known repeatedly sampled individuals per range (Beecher, 1989; Linhart et al., 2019). We used five individuals per range, recorded at a single site-year in the native range (site 1145 in 2017) and recorded at three sites in a

single city-year (Austin, Texas in 2019) in the invasive range. These individuals were used to calculate HS because they represented similar patterns of dispersion in acoustic space per range (Appendix, Fig. A2), and because we did not repeatedly sample five individuals at any single site in the invasive range. HS was calculated by performing PCA on 88 descriptive statistics of Mel-frequency cepstral coefficients (MFCC) (see Appendix, Obtaining predictors for machine learning) and second harmonic frequency contours with five calls per individual. We used MFCC because these measurements summarized frequency modulation patterns as well as other aspects of acoustic structure, including timbre and absolute frequency, that may arise from individual differences in vocal morphology and contribute to individual vocal signatures. We used the same fifty calls to calculate HS from MFCC and frequency contours per range (see Appendix, Calculation of Beecher's statistic). HS was calculated for frequency contours after dropping five points on either end of each contour and without spline interpolation. We estimated the number of possible unique individual signatures, given the amount of individual identity content per range, as 2^{HS} (Beecher, 1989; Linhart et al., 2019).

Independent Effects of Habitat and Range on Acoustic Structure of Contact Calls

As invasive range monk parakeets were recorded in urban habitats, but native range parakeets were largely recorded in agro-interface habitats, the analyses above comparing acoustic structure between ranges included a partially confounded comparison between habitat types. We used a subsample of the full data set of calls that represented broad geographical sampling in each range to assess the independent effects of range and habitat on contact call structure. As the full data set contained contact calls recorded at four native range urban sites, we selected four native range agro-interface sites and four invasive range urban sites for subsequent analysis. Calls at the four invasive range sites were randomly subsampled to yield sample sizes more comparable to sites selected from the native range (see Appendix, Effects of habitat and range on acoustic measurements). Native range agro-interface, native range urban and invasive range urban habitats were represented by 82, 48 and 80 calls, respectively (210 calls total).

We assessed patterns of acoustic variation across these three range–habitat types by PCA on the 27 spectral acoustic measurements used above. We used the resulting principal components to visualize separation among range–habitats in low-dimensional acoustic space. We evaluated the independent effects of habitat and range by calculating Cliff's delta with bootstrapped 95% CIs from two overall comparisons: we compared native range urban calls to native range agro-interface calls (i.e. the effect of habitat without the confound of range, with agro-interface habitat as the baseline) and compared invasive range urban calls to native range urban calls (i.e. the effect of range without the confound of habitat, with the native range as the baseline). We calculated Cliff's delta for the 27 spectral acoustic measurements with the subsampled calls described above but used a smaller data set of 24 calls to assess the independent effects of habitat and range on the three customized frequency modulation measurements (see Appendix, Effects of habitat and range on acoustic measurements).

Ethical Note

Recording parakeet vocalizations was a noninvasive sampling method. Recordists obtained calls from individuals flying in and out of nesting sites, or perched near nests, during parakeets' normal daily activities, usually within 5–10 m of birds. Several native range individuals were trapped and marked in previous work. Birds were extracted from traps and processed as quickly as possible to reduce stress, using a previously published marking method that has been successfully used for this species, as described in Smith-Vidaurre et al. (2020). Birds that showed signs of high stress during trapping were not marked. Marked individuals were monitored for high stress prior to release and were recorded similarly to unmarked birds for several days after marking. This research was conducted under an approved Institutional Animal Care and Use protocol (IACUC no. 2017-006, New Mexico State University, U.S.A.) and an animal care and use protocol approved by la Comisión de Ética en el Uso de Animales (CEUA no. 240011-002512-17, la Universidad de la República, Uruguay).

RESULTS

Proxies of Local Population Size in Each Range

We observed a median of 19.5 nests (IQR: 24.25) over 20 native range sites and 4.00 nests (IQR: 6.00) over 17 invasive range sites (Fig. 1). The reduced data set employed for Mann–Whitney–Wilcoxon tests, in which 13 invasive range sites were retained to meet the assumption of independent samples, exhibited the same median and IQR for the number of nests as the full data set (in which some invasive range sites had been sampled in more than one year). The maximum number of nests observed at a given site was an order of magnitude greater in the native range compared to the invasive range (Fig. 1, Appendix, Table A2). Mann–Whitney–Wilcoxon tests conducted with 33 total sites (20 native range sites and 13 invasive range sites) showed that the distributions of total nest estimates differed significantly between the two ranges (difference in Mann–Whitney location between ranges: 14 [95% CI: 7, 26], $Z = 4.21$, $P < 0.0001$).

We identified a trend towards lower nest densities in the invasive range. Nest densities were greater in the native range (median: 29.05 nests/ha, IQR: 29.34) than the invasive range (median: 10.81 nests/ha, IQR: 14.39) (Fig. 1). However nest densities were not significantly different between ranges (difference in Mann-Whitney location: 8.42 [95% CI: -7.63, 28.94], $Z = 0.92$ and $P = 0.38$), likely due to large variation in both ranges (Fig. 1). This trend of reduced nest densities was not due to a difference in the size of the areas we surveyed for nests per range, as site areas were similar between 16 native range sites (median: 0.86 ha, IQR: 0.78) and 10 invasive range sites (median: 0.84 ha, IQR: 2.44) (Fig. 1), and the difference between ranges was not significant (difference in Mann–Whitney location: 0.37 [95% CI: -0.28, 1.07], $Z = 1.47$, $P = 0.15$).

Maximum Flock Sizes Observed in Each Range

The maximum flock sizes we estimated across behavioural contexts during fieldwork were larger in the native range (median: 75.0 individuals, IQR: 50.5) compared to the invasive range (median: 30.0 individuals, IQR: 11.2). Maximum flock size estimates were more than twice as large on average for the native range compared to the invasive range. This was a conservative difference, given the hundreds of birds observed foraging in corn or soy bean fields in the department of Colonia, Uruguay, where monk parakeets exhibit some of the highest population densities in the country (G. Smith-Vidaurre, personal observation). Maximum estimated flock sizes differed significantly between ranges (difference in Mann–Whitney location: 53, $Z = 2.38$, $P = 0.03$). A 95% CI was not computed for this statistical test due to low sample sizes (4 observations were used per range to meet the assumption of nonindependence).

Frequency Modulation Patterns Compared between Ranges

Native and invasive range calls exhibited visible differences in frequency modulation patterns and other aspects of acoustic structure (Fig. 2a). Visible structural differences among ranges were consistent with high classification accuracy of calls back to each range by supervised random forests across model training (91.09%), validation (91.99%) and prediction steps (87.59%) (Appendix, Table A6), as well as the differentiation observed between ranges in random forests acoustic space (Fig. 2b). Frequency modulation patterns contributed significantly to structural differences between ranges. Invasive range calls exhibited fewer frequency modulation peaks, lower modulation rates and shallower maximum peak–trough slopes (Fig. 3b). The effect of range was large and statistically significant for the number of peaks (Cliff's delta: -0.69 [95% CI: -0.82, -0.49]), the peak–trough slope (Cliff's delta: 0.69 [95% CI: 0.48, 0.83]) and the modulation rate (Cliff's delta: -0.63 [95% CI: -0.79, -0.41]; Appendix, Table A7). Invasive range calls also exhibited significantly greater standard deviation of frequency (Cliff's delta: 0.78 [95% CI: 0.61, 0.89]), spectral flatness (Cliff's delta: 0.58 [95% CI: 0.35, 0.75]) and entropy (Cliff's delta: 0.51 [95% CI: 0.27, 0.69]) compared to native range calls (Appendix, Table A7). The

trend of simpler frequency modulation patterns identified in invasive range calls was consistent over the 15-year sampling period in the invasive range (Appendix, Fig. A1).

Individual Identity Content in Native and Invasive Range Calls

Beecher's statistic was lower for invasive range calls. This reduced individual identity content yielded fewer distinctive individual signatures in the invasive range acoustic space compared to native range calls. Trends for Beecher's statistic and the number of possible unique individual signatures were similar between descriptive statistics of MFCC, as well as second harmonic frequency contours employed to measure the complexity of frequency modulation patterns (Fig. 3c, Table 1).

Effects of Habitat and Range on Frequency Modulation Patterns

Native range agro-interface calls demonstrated separation in acoustic space from native and invasive range urban calls when PCA was performed on 27 standard spectral acoustic measurements (Appendix, Fig. A3). We asked which acoustic measurements displayed the largest effects of habitat or range by calculating Cliff's delta from two overall pairwise comparisons, which allowed us to address the partial confound of habitat in our data set. In these analyses, the effect of habitat (independent of range) was obtained by comparing native range urban calls to native range agro-interface calls, while the effect of range (independent of habitat) was obtained by comparing invasive range urban calls to native range urban calls. Ten spectral acoustic measurements displayed significant effects of habitat, while 12 spectral acoustic measurements showed significant effects of range (Appendix, Table A8), and two different customized frequency modulation measurements displayed significant effects of either habitat and/or range (Appendix, Table A9).

Five temporal acoustic measurements exhibited large effects of habitat: duration (Cliff's delta: -0.66 [95% CI: -0.79, -0.47]), time entropy (Cliff's delta: 0.66 [95% CI: 0.47, 0.80]), third quartile time (Cliff's

delta: -0.64 [95% CI: -0.78, -0.45]), time interquartile range (Cliff's delta: -0.60 [95% CI: -0.75, -0.41]) and median time (Cliff's delta: -0.48 [95% CI: -0.64, -0.28]) as well as two of the three customized frequency modulation measurements, obtained with a smaller data set of calls: the number of peaks (Cliff's delta: -0.77 [95% CI: -0.92, -0.16]) and modulation rate (Cliff's delta: -0.62 [95% CI: -1.00, -0.06]). Native range agro-interface calls therefore exhibited significantly longer duration, more frequency modulation peaks and higher modulation rates than native range urban calls. If parakeets were avoiding masking by low-frequency noise in urban habitats, we expected to identify increased pitch in urban calls. However, measurements related to pitch (e.g. first quartile frequency and frequency interquartile range) did not show large effects of habitat (Fig. 4, Appendix, Tables A8, A9).

The largest effects of range were identified for five different spectral acoustic measurements in the frequency domain: standard deviation of frequency (Cliff's delta: 0.60 [95% CI: 0.43, 0.73]), dominant frequency range (Cliff's delta: 0.57 [95% CI: 0.37, 0.72]), minimum dominant frequency (Cliff's delta: -0.55 [95% CI: -0.70, -0.38]), end dominant frequency (Cliff's delta: -0.51 [95% CI: -0.68, -0.29]) and spectral entropy (Cliff's delta: 0.48 [95% CI: 0.28, 0.63]) as well as two of the three customized frequency modulation measurements that were obtained with a smaller data set of calls: peak–trough slope (Cliff's delta: 0.91 [95% CI: 0.25, 1.00]) and the number of peaks (Cliff's delta: -0.66 [95% CI: -0.92, -0.16]). The standard deviation of frequency and spectral entropy also exhibited large and significant effects of range in our comparison above where we did not account for the partial confound of habitat type (Fig. 3, Appendix, Table A7). Native range urban calls therefore displayed significantly higher minimum and end dominant frequencies as well as a narrower range of dominant frequencies, lower spectral entropy, steeper frequency modulation peak–trough slopes and more frequency modulation peaks compared to invasive range urban calls (Fig. 4, Appendix, Tables A8, A9). Overall, invasive range urban calls displayed the simplest frequency modulation patterns compared to native range calls in both habitats (Fig. 4).

DISCUSSION

We compared local population sizes, social group sizes and contact call structure between native and invasive range monk parakeets to ask whether the putative use of vocal learning for individual recognition was sensitive to changes in the social environment following invasion. Our two proxies for local population size, nest numbers and nest densities at nesting sites, both indicated that populations in the invasive range were smaller than in the native range. Smaller local population sizes should limit the maximum social group sizes that individuals experience in other social contexts, such as foraging, which was supported by our estimates of smaller maximum flock sizes in the invasive range. Frequency modulation patterns were significantly simpler and contained less individual identity content in invasive range calls, indicating that the structure of individual signatures in learned calls was sensitive to altered social environments in the invasive range. Call structure also differed significantly between calls recorded at native range agro-interface sites and calls recorded at urban sites in each range. However, we did not identify evidence of urban parakeets increasing the pitch of contact calls to avoid masking by low-frequency anthropogenic noise. Instead, we identified a simplification of frequency modulation patterns in urban calls and changes in other acoustic measurements related to frequency modulation. Our results suggest that monk parakeets use vocal learning for individual recognition and that this putative use of vocal learning for social recognition is sensitive to reductions in local population size associated with the invasion of novel ranges or urban habitats. Whether receivers use individual signatures in contact calls for individual vocal recognition will be important to evaluate in future work with playback experiments.

Individual Signatures and Individual Identity Content in Contact Calls

Simpler frequency modulation patterns, resulting in simpler individual vocal signatures, may be due to smaller group sizes and hence relaxed selection for individual vocal distinctiveness in the invasive range. Smaller invasive population sizes can occur during the early stages of invasion (Duncan et al., 2003; Estoup et al., 2016), and small population sizes could persist post-invasion in the absence of significant population growth

over time. Indeed, although nesting site areas were similar between ranges, we observed fewer nests and generally lower nest densities at invasive range sites, as well as smaller maximum flock sizes, consistent with previous reports of slowed population growth or population declines in invasive range populations in the U.S. (Pruett-Jones et al., 2012; Pruett-Jones & Tarvin, 1998). The differences in site areas and nest densities between ranges were not statistically significant, but in sum, these variables showed a consistent pattern of fewer nests distributed over similar areas in the invasive range compared to the native range. Fewer nests, lower nest densities and smaller maximum flock sizes were in line with our expectations of altered social environments following invasion, in which invasive range populations likely experience fewer opportunities for social interactions over similar geographical areas compared to larger and more contiguous populations in the native range. Fewer nests and lower nest densities at invasive range sites were unlikely to result from pest control activities, as such methods are undertaken in each range, and parakeets rebuild nests in response to such disturbance (see Appendix, Pest control and proxies of local population size). We do not know whether social dynamics change following invasion, but this seems plausible given smaller local population sizes, smaller social group sizes and increased geographical isolation of invasive range sites in cities compared to the high population contiguity observed in agro-interface habitats in the native range (G. Smith-Vidaurre, personal observation).

The reduced individual identity content we identified in invasive range calls is also consistent with relaxed selection for individual recognition in smaller populations. Beecher's statistic (HS) calculated with descriptive statistics of Mel-frequency cepstral coefficients estimated 7.67 unique individual signatures for the native range versus 5.62 for the invasive range, while HS calculated from frequency contours estimated 4.20 versus 1.19 unique signatures. Future work could manipulate social group size as well as social dynamics to ask whether vocal learning facilitates altering individual signatures to match changes in social group complexity over short timescales. Monk parakeets exhibit high fission–fusion fluidity (Hobson et al., 2014), but how social dynamics might influence individual recognition remains an open question. Fission–fusion dynamics could differ between ranges, in turn influencing the frequency of repeated social interactions that require individual vocal recognition.

We also identified simpler frequency modulation patterns in calls at urban sites in the native range. We did not identify an increase in the pitch of urban calls however, which was expected as a response to masking by low-frequency anthropogenic noise, given findings with other vocal learning birds (Halfwerk et al., 2011; Halfwerk & Slabbekoorn, 2009, 2014; Hu et al., 2010). These results suggest that the social environment of monk parakeets is altered in urban habitats in a way that influences individual vocal recognition. Simpler frequency modulation patterns in urban calls could arise if urban populations were more geographically isolated than native range agro-interface populations. Monk parakeets roost in their stick nests throughout the year (Buhrman-Deever et al., 2007; Eberhard, 1998), which ties individuals to a particular nesting site more than other parrots that nest in secondary cavities and roost in separate locations (Bradbury & Balsby, 2016; Buhrman-Deever et al., 2007). Green spaces in urban areas are, by definition, more geographically isolated than those in agro-interface habitats (Goddard et al., 2010). It is possible that urban parakeets are less likely to interact with individuals from other nesting sites than are individuals in agro-interface habitats, which would limit their social interactions. We observed the same effect on call structure in invasive range populations, which were sampled at urban sites. Overall, our results indicate that the simplification of individual signatures in contact calls is associated with reductions in population size following invasion, as well as habitat differences among populations, and such simplification may be due to reduced social demands for individual vocal recognition. Recent work documented a similar link between the social environment and simplification of learned vocalizations in critically endangered regent honeyeaters, *Anthochaera phrygia*, although in the context of mate attraction. In the honeyeaters, reduced population density appears to contribute to a paucity of conspecific tutors from which juvenile males can learn songs with sufficient species-specific vocal complexity to attract mates (Crates et al., 2021).

Frequency Modulation Patterns in Invasive Range Calls and Possible Founder Effects

The structural differences we identified in contact calls between ranges could be due to an effect

of withdrawal of learning during population founding. This founder effect has been suggested to occur when invasive populations are established by juvenile and/or captive birds that lacked adult tutors and thus developed atypical calls (Lachlan et al., 2013; Parker, Anderson, Jenkins, & Brunton, 2012; Thielcke, 1973). We consider this alternative less likely, because changes in acoustic structure were concentrated on aspects of frequency modulation rather than distributed across all acoustic measurements, as would be expected if individuals produced contact calls that were atypical for this species. Furthermore, these changes were seen across multiple, presumably independent, invasions in five different states in the U.S. Withdrawal of learning would have had to occur five times in a similar fashion to yield the results reported here.

Another possibility is that structural differences could be due to genetic bottlenecks, a common outcome of biological invasions (Bock et al., 2015; Dlugosch & Parker, 2008). However, although genetic bottlenecks were identified in invasive range populations in a separate study, these genetic bottlenecks were weak (Smith-Vidaurre, 2020), a further indication that the simpler individual signatures identified here were not driven by a strong reduction in neutral genetic diversity post-invasion. Finally, the structural changes we identified between ranges did not arise from differences in regional dialects. Native range populations do not exhibit regional dialects in contact calls (Smith-Vidaurre et al., 2020), and in a complementary study, we did not identity patterns of acoustic variation in invasive range populations consistent with regional dialects (Smith-Vidaurre et al., 2021).

Effects of Frequency Modulation Patterns on Individual Vocal Recognition

Frequency modulation patterns can be altered by learning and can yield distinctive individual signatures that facilitate individual vocal recognition in vocal learning taxa, as documented in bottlenose dolphins, *Tursiops truncatus*, and green-rumped parrotlets, *Forpus passerinus* (Berg et al., 2011; Fripp et al., 2005; Janik et al., 2006). However, frequency modulation patterns are also used for individual vocal recognition by taxa that rely on acoustic signals with presumably stronger genetic encoding. For instance, simpler frequency

modulation patterns have been identified in colonially breeding taxa that use acoustic signals for individual vocal recognition but do not appear to acquire such signals by social learning. King penguins, *Aptenodytes patagonicus*, live in large colonies in which the concurrent production of acoustic signals by many individuals results in high jamming of signallers' calls and therefore high receiver uncertainty (Jouventin, Aubin, & Lengagne, 1999). King penguin chicks use frequency modulation patterns in parents' calls for individual recognition (Jouventin et al., 1999). A comparative study subsequently demonstrated that frequency modulation is used for individual recognition by two non-nesting penguin species that locate kin by acoustic cues alone, but not by two nesting species, in which nest location is important for locating family members (Jouventin & Aubin, 2002). Similar results have been identified in swallows, in which colonially breeding species use acoustic cues to recognize offspring, but solitary species or species that live in smaller social groups do not (Beecher, Medvin, Stoddard, & Loesche, 1986). In addition, in the colonially breeding swallows, offspring exhibited individually distinctive calls with more complex frequency modulation patterns than in solitary species (Beecher et al., 1986).

How vocal learning facilitates individual recognition will be an interesting direction for future research. When a given species relies on individual vocal recognition to mediate social interactions, vocal learning may allow individuals to modify the complexity of their frequency modulation patterns to match changes in the complexity of their social environment and could also allow individuals to produce signatures that are more individually distinctive compared to genetically encoded acoustic signals (Nowicki et al., 2014). The complexity of social environments can be influenced by other aspects of socioecology aside from breeding behavior. For instance, in parrots, it has been suggested that species' tracking of transient food resources should influence the social complexity of different species, which could in turn influence variation in socially learned acoustic signals (Bradbury et al., 2016), an idea that could be tested in subsequent research. The distribution of resources within habitats has been proposed as a major driver of variation in social environments more generally across taxa (He, Maldonado-Chaparro, & Farine, 2019), and monk parakeets could be a useful system in which to test this idea.

Costs and Constraints in Individual Recognition Systems

Simpler individual signatures in learned acoustic signals may be favoured due to cognitive costs, lower costs associated with errors in individual recognition, or may arise from developmental constraints. In larger social groups, receivers should experience greater cognitive costs of discriminating among more individuals while simultaneously processing individual signatures against a noisier background. Such costs are thought to include the energy needed to maintain neural structures associated with learning and memory, both of which are critical for individual recognition systems (Injaian & Tibbetts, 2014). Signallers may experience costs of learning to encode more distinctive individual signatures through complex structural variation. In the monk parakeet system, all individuals produce contact calls and are also potential receivers of other individuals' calls; therefore, all individuals should experience costs of both receiver perception and vocal production (Sewall et al., 2016). As the perception and production of complex individual signatures should pose greater cognitive burdens, simpler individual signatures should be present in smaller groups in which accurate recognition is possible without such complexity.

Simpler or less informative signaller traits should also be favoured when the costs of errors in individual recognition are lower (Tibbetts, Liu, Laub, & Shen, 2020). In monk parakeets, the cost of errors in individual recognition could be related to nest territoriality, a factor that may select for individual recognition systems (Tibbetts & Dale, 2007). Individuals invest a large amount of their time in building and maintaining nests (Burgio et al., 2020) and have been reported to fight with individuals in neighbouring nests (Burgio et al., 2020) and steal twigs from other nests (Eberhard, 1998). Individuals in larger local populations may therefore experience greater costs of failing to recognize conspecific nest competitors. Both cognitive costs and costs of errors could be working in the smaller populations found in the invasive range to yield simpler signatures.

Simpler individual signatures may also reflect developmental constraints in receiver perception and signaller production. Although parrots are considered open-ended vocal learners (Bradbury et al., 2016), we do not know whether auditory perception remains sensitive throughout adulthood (Dooling, Leek, Gleich, &

Dent, 2002). In monk parakeets, signaller production and receiver perception of individual signatures may be constrained by local population densities experienced during sensitive developmental periods. Finally, other forms of social recognition may be at play in this system that were not captured with the current sampling, such as rapid directional changes in call convergence that have been identified in other parrot species (Balsby & Bradbury, 2009; Scarl & Bradbury, 2009; Wanker, Sugama, & Prinage, 2005), which could be assessed with field experiments or social groups in short-term captivity. The findings we present here on the complexity of individual signatures produced by an invasive parrot contribute to a growing foundation for future work on how vocal learning is used for individual recognition in dynamic social groups.

Data Accessibility

Annotated code and knitted Rmarkdown output supporting this article are available on GitHub (http://github.com/gsvidaurre/simpler-signatures-post-invasion, DOI: 10.5281/zenodo.4993536). Data that can be used to reproduce results were deposited in figshare: https://doi.org/10.6084/m9.figshare.14811636.v1.

Funding

This research was supported by a Fulbright Study/Research grant to G.S.V., a New Mexico State University Honors College scholarship to Clara Hansen, an American Ornithologists' Union Carnes Award to G.S.V., Experiment.com crowdfunding led by G.S.V. and Dr Kevin Burgio, a donation to G.S.V. from Michael and Susan Achey, a New Mexico State University Whaley Field Award to G.S.V., and Maximizing Access to Research Careers (MARC) funding to V.P.M. (Biomedical Research Training for Honor Undergraduates supported by the U.S. National Institutes of Health/National Institute of General Medical Sciences (NIH/NIGMS 5T34GM007667)). G.S.V. was also supported by a NSF Postdoctoral Research Fellowship (grant number 2010982) while working on this research.

Competing Interests

We declare no conflicts of interest associated with authorship or publication of this article.

Author Contributions

G.S.V. helped design the study, performed fieldwork, curated and analysed data and was the primary author of the manuscript. V.P.M. performed fieldwork, curated and analysed data and reviewed the manuscript. T.F.W. helped design the study and contributed to fieldwork, data analysis and writing the manuscript.

Acknowledgments

We thank Clara Hansen for help trapping, marking and recording parakeets in Uruguay as well as Tania Molina for help with fieldwork in Uruguay. We thank numerous additional people for their support throughout native range fieldwork as acknowledged in Smith-Vidaurre et al. (2020), and would like to particularly thank Dr Enrique Lessa, Dr Bettina Tassino, Dr Ivanna Tomasco, Gabino Suanes, Claudia Perez, Dr Ethel Rodríguez and Instituto Nacional de Investigación Agropecuaria (INIA) directors Dario Hirigoyen and Santiago Cayota for their help with fieldwork logistics in Uruguay. We are also grateful to Zoë Amerigian and Alexandra Bicki for their help during 2019 fieldwork and to Dr Susannah Buhrman-Deever for providing data. This manuscript benefited from discussion with Dr Alejandro Salinas-Melgoza, Dr Elizabeth Hobson and Dominique Hellmich. Finally, we are grateful to two anonymous referees who helped us greatly improve earlier versions of this manuscript.

References

Allen, M., Poggiali, D., Whitaker, K., Marshall, T.R., & Kievit, R.A. (2019). Raincloud plots: A multi-platform tool for robust data visualization. *Wellcome Open Research*, *4*(63), 1–40. https://doi.org/10.12688/wellcomeopenres.15191.1

Araya-Salas, M., & Smith-Vidaurre, G. (2017). warbleR: An R package to streamline analysis of animal acoustic signals. *Methods in Ecology and Evolution*, *8*(2), 184–191. https://doi.org/10.1111/2041-210X.12624

Avery, M.L., Tillman, E.A., Keacher, K.L., Arnett, J.E., & Lundy, K.J. (2012). Biology of invasive monk parakeets in south Florida. *Wilson Journal of Ornithology*, *124*(3), 581–588. https://doi.org/10.1676/11-188.1

Balsby, T.J.S., & Bradbury, J.W. (2009). Vocal matching by orange-fronted conures (*Aratinga canicularis*). *Behavioural Processes*, *82*(2), 133–139. https://doi.org/10.1016/j.beproc.2009.05.005

Beecher, M.D. (1989). Signaling systems for individual recognition: An information theory approach. *Animal Behaviour*, *38*(2), 248–261. https://doi.org/10.1016/S0003-3472(89)80087-9

Beecher, M.D., Medvin, M.B., Stoddard, P.K., & Loesche, P. (1986). Acoustic adaptations for parent–offspring recognition in swallows. *Experimental Biology*, *45*(3), 179–193.

Berg, K.S., Delgado, S., Cortopassi, K.A., Beissinger, S.R., & Bradbury, J.W. (2012). Vertical transmission of learned signatures in a wild parrot. *Proceedings of the Royal Society B: Biological Sciences*, *279*(1728), 585–591. https://doi.org/10.1098/rspb.2011.0932

Berg, K.S., Delgado, S., Okawa, R., Beissinger, S.R., & Bradbury, J.W. (2011). Contact calls are used for individual mate recognition in free-ranging green-rumped parrotlets, *Forpus passerinus*. *Animal Behaviour*, *81*(1), 241–248. https://doi.org/10.1016/j.anbehav.2010.10.012

Bock, D.G., Caseys, C., Cousens, R.D., Hahn, M.A., Heredia, S.M., Hubner, S., Turner, K.G., Whitney, K.D., & Rieseberg, L.H. (2015). What we still don't know about invasion genetics. *Molecular Ecology*, *24*(9), 2277–2297. https://doi.org/10.1111/mec.13032

Borchers, H.W. (2019). *pracma: Practical numerical math functions* (R package version 2.2.9). https://cran.r-project.org/package=pracma

Bradbury, J.W., & Balsby, T.J.S. (2016). The functions of vocal learning in parrots. *Behavioral Ecology and Sociobiology*, *70*, 293–312. https://doi.org/10.1007/s00265-016-2068-4

Breiman, L. (2001). Random forests. *Machine Learning*, *45*, 5–32. https://doi.org/10.1007/9781441993267_5

Buhrman-Deever, S.C., Rappaport, A.R., & Bradbury, J.W. (2007). Geographic variation in contact calls of feral North American populations of the monk parakeet. *Condor*, *109*(2), 389–398. https://doi.org/10.1525/boom.2013.3.4.67.B

Burgio, K.R., van Rees, C.B., Block, K.E., Pyle, P., Patten, M.A., Spreyer, M.F., & Bucher, E.H. (2020). Monk parakeet (*Myiopsitta monachus*) (version 1.0). In P. G. Rodewald (Ed.), *Birds of the world*. Ithaca, NY: Cornell Lab of Ornithology. https://doi.org/https://doi.org/10.2173/bow.monpar.01

Chen, L.T., & Chao-Ying, J.P. (2015). The sensitivity of three methods to nonnormality and unequal variances in interval estimation of effect sizes. *Behavior Research Methods*, *47*(1), 107–126. https://doi.org/10.3758/s13428-014-0461-3

Cliff, N. (1996). *Ordinal methods for behavioral data analysis*. New York, NY: Psychology Press.

Cornell Lab of Ornithology Bioacoustics Research Program. (2014). *Raven Pro: Interactive sound analysis software*. Ithaca, NY: Cornell Lab of Ornithology.

Crates, R., Langmore, N., Ranjard, L., Stojanovic, D., Rayner, L., Ingwersen, D., & Heinsohn, R. (2021). Loss of vocal culture and fitness costs in a critically endangered songbird. *Proceedings of the Royal Society B, 288*(1947), 20210225. https://doi.org/10.1098/rspb.2021.0225

Davis, A.Y., Malas, N., & Minor, E.S. (2014). Substitutable habitats? The biophysical and anthropogenic drivers of an exotic bird's distribution. *Biological Invasions*, *16*(2), 415–427. https://doi.org/10.1007/s10530-013-0530-z

Dlugosch, K.M., & Parker, I.M. (2008). Founding events in species invasions: Genetic variation, adaptive evolution, and the role of multiple introductions. *Molecular Ecology*, *17*(1), 431–449.

https://doi.org/10.1111/j.1365-294X.2007.03538.x

Dooling, R.J., Leek, M.R., Gleich, O., & Dent, M.L. (2002). Auditory temporal resolution in birds: Discrimination of harmonic complexes. *Journal of the Acoustical Society of America*, *112*(2), 748–759. https://doi.org/10.1121/1.1494447

Duncan, R.P., Blackburn, T.M., & Sol, D. (2003). The ecology of bird introductions. *Annual Review of Ecology, Evolution, and Systematics*, *34*, 71–98. https://doi.org/10.1146/annurev.ecolsys.34.011802.132353

Eberhard, J.R. (1998). Breeding biology of the monk parakeet. *Wilson Bulletin*, *110*(4), 463–473.

Edelaar, P., Roques, S., Hobson, E.A., Gonçalves Da Silva, A., Avery, M.L., Russello, M.A., Senar, J.C., Wright, T.F., Carrete, M., & Tella, J.L. (2015). Shared genetic diversity across the global invasive range of the monk parakeet suggests a common restricted geographic origin and the possibility of convergent selection. *Molecular Ecology*, *24*(9), 2164–2176. https://doi.org/10.1111/mec.13157

Estoup, A., Ravigné, V., Hufbauer, R., Vitalis, R., Gautier, M., & Facon, B. (2016). Is there a genetic paradox of biological invasion? Annual Review of Ecology, Evolution, and Systematics, 47, 51–72. https://doi.org/10.1146/annurev-ecolsys-121415-032116

Friedman, J.H. (2001). Greedy function approximation: A gradient boosting machine. *Annals of Statistics*, *29*(5), 1189–1232. https://doi.org/10.1214/aos/1013203451

Fripp, D., Owen, C., Quintana-Rizzo, E., Shapiro, A., Buckstaff, K., Jankowski, K., Wells, R., & Tyack, P. (2005). Bottlenose dolphin (*Tursiops truncatus*) calves appear to model their signature whistles on the signature whistles of community members. *Animal Cognition*, *8*(1), 17–26. https://doi.org/10.1007/s10071-004-0225-z

Goddard, M.A., Dougill, A.J., & Benton, T.G. (2010). Scaling up from gardens: Biodiversity conservation in urban environments. *Trends in Ecology & Evolution*, *25*(2), 90–98. https://doi.org/10.1016/j.tree.2009.07.016

Greenwell, B., Boehmke, B., Cunningham, J., & GBM-Developers. (2019). *gbm: Generalized boosted regression models* (R package version 2.1.5). https://cran.r-project.org/package=gbm

Halfwerk, W., Bot, S., Buikx, J., van der Velde, M., Komdeur, J., ten Cate, C., & Slabbekoorn, H. (2011). Low-frequency songs lose their potency in noisy urban conditions. *Proceedings of the National Academy of Sciences of the United States of America*, *108*(35), 14549–14554. https://doi.org/10.1073/pnas.1109091108

Halfwerk, W., & Slabbekoorn, H. (2009). A behavioural mechanism explaining noise-dependent frequency use in urban birdsong. *Animal Behaviour*, *78*(6), 1301–1307. https://doi.org/10.1016/j.anbehav.2009.09.015

Halfwerk, W., & Slabbekoorn, H. (2014). The impact of anthropogenic noise on avian communication and fitness. In D. Gil & H. Brumm (Eds.), *Avian urban ecology* (1st ed., pp. 84–97). Oxford, U.K.: Oxford University Press.

He, P., Maldonado-Chaparro, A.A., & Farine, D.R. (2019). The role of habitat configuration in shaping social structure: A gap in studies of animal social complexity. *Behavioral Ecology and Sociobiology*, *73*(1), 1–14. https://doi.org/10.1007/s00265-018-2602-7

Hess, M.R., & Kromrey, J.D. (2004). [Robust confidence intervals for effect sizes: A comparative study of Cohen's *d* and Cliff's delta under non-normality and heterogeneous variances]. Paper presented at the annual meeting of the American Educational Research Association, San Diego, 12–16 April 2004.

Hobson, E.A., Avery, M.L., & Wright, T.F. (2014). The socioecology of monk parakeets: Insights into parrot social complexity. *Auk*, *131*, 756–775. https://doi.org/10.1642/AUK-14-14.1

Hu, Y., & Cardoso, G.C. (2010). Which birds adjust the frequency of vocalizations in urban noise? *Animal Behaviour*, *79*(4), 863–867. https://doi.org/10.1016/j.anbehav.2009.12.036

Injaian, A., & Tibbetts, E.A. (2014). Cognition across castes: Individual recognition in worker *Polistes fuscatus* wasps. *Animal Behaviour*, *87*, 91–96. https://doi.org/10.1016/j.anbehav.2013.10.014

Janik, V.M., Sayigh, L.S., & Wells, R.S. (2006). Signature whistle shape conveys identity information to bottlenose dolphins. *Proceedings of the National Academy of Sciences of the United States of America*, *103*(21), 8293–8297. https://doi.org/10.1073/pnas.0509918103

Janik, V.M., & Slater, P.J.B. (2000). The different roles of social learning in vocal communication. *Animal*

Behaviour, *60*(1), 1–11. https://doi.org/10.1006/anbe.2000.1410

Jouventin, P., & Aubin, T. (2002). Acoustic systems are adapted to breeding ecologies: Individual recognition in nesting penguins. *Animal Behaviour*, *64*(5), 747–757. https://doi.org/10.1006/anbe.2002.4002

Jouventin, P., Aubin, T., & Lengagne, T. (1999). Finding a parent in a king penguin colony: The acoustic system of individual recognition. *Animal Behaviour*, *57*(6), 1175–1183. https://doi.org/10.1006/anbe.1999.1086

Kuhn, M. (2020). *caret: Classification and regression training* (R package version 6.0-86). https://cran.r-project.org/package=caret

Lachlan, R.F., Verzijden, M.N., Bernard, C.S., Jonker, P.P., Koese, B., Jaarsma, S., Spoor, W., Slater, P.J.B., & ten Cate, C. (2013). The progressive loss of syntactical structure in bird song along an island colonization chain. *Current Biology*, *23*(19), 1896–1901. https://doi.org/10.1016/j.cub.2013.07.057

Linhart, P., Osiejuk, T.S., Budka, M., Salek, M., Spinka, M., Policht, R., Syrova, M., & Blumstein, D.T. (2019). Measuring individual identity information in animal signals: Overview and performance of available identity metrics. *Methods in Ecology and Evolution*, *10*(9), 1558–1570. https://doi.org/10.1111/2041-210X.13238

Nowicki, S., & Searcy, W.A. (2014). The evolution of vocal learning. *Current Opinion in Neurobiology*, *28*, 48–53. https://doi.org/10.1016/j.conb.2014.06.007

Parker, K.A., Anderson, M.J., Jenkins, P.F., & Brunton, D.H. (2012). The effects of translocation-induced isolation and fragmentation on the cultural evolution of bird song. *Ecology Letters*, *15*(8), 778–785. https://doi.org/10.1111/j.1461-0248.2012.01797.x

Pollard, K.A., & Blumstein, D.T. (2011). Social group size predicts the evolution of individuality. *Current Biology*, *21*(5), 413–417. https://doi.org/10.1016/j.cub.2011.01.051

Pranty, B. (2009). Nesting substrates of monk parakeets (*Myiopsitta monachus*) in Florida. *Florida Field Naturalist*, *37*(2), 51–57.

Pruett-Jones, S., Appelt, C.W., Sarfaty, A., van Vossen, B., Leibold, M.A., & Minor, E.S. (2012). Urban parakeets in northern Illinois: A 40-year perspective. *Urban Ecosystems*, *15*(3), 709–719.

https://doi.org/10.1007/s11252-011-0222-3

Pruett-Jones, S., & Tarvin, K.A. (1998). Monk parakeets in the United States: Population growth and regional patterns of distribution. In R. O. Baker & A. C. Crabb (Eds.), *Proceedings of the 18th Vertebrate Pest Conference* (pp. 55–58). Davis, CA: University of California Press. Retrieved from https://digitalcommons.unl.edu/vpc18/67/

R Core Team. (2018). *R: A language and environment for statistical computing*. Vienna, Austria. https://www.r-project.org/

Romano, J., Kromrey, J.D., Coraggio, J., Skowronek, J., & Devine, L. (2006). [Exploring methods for evaluating group differences on the NSSE and other surveys: Are the *t*-test and Cohen's *d* indices the most appropriate choices?] Paper presented at the annual meeting of the Southern Association for Institutional Research, 14–17 October 2006, Arlington, Virginia (pp. 14–17).

Russello, M.A., Avery, M.L., & Wright, T.F. (2008). Genetic evidence links invasive monk parakeet populations in the United States to the international pet trade. *BMC Evolutionary Biology*, *8*, 217. https://doi.org/10.1186/1471-2148-8-217

Scarl, J.C., & Bradbury, J.W. (2009). Rapid vocal convergence in an Australian cockatoo, the galah *Eolophus roseicapillus*. *Animal Behaviour*, *77*(5), 1019–1026. https://doi.org/10.1163/156853909X427696

Sewall, K.B., Young, A.M., & Wright, T.F. (2016). Social calls provide novel insights into the evolution of vocal learning. *Animal Behaviour*, *120*, 163–172. https://doi.org/10.1016/j.anbehav.2016.07.031

Smith-Vidaurre, G. (2020). *Patterns of genetic and acoustic variation in a biological invader* (Ph.D. thesis). Las Cruces, NM: New Mexico State University.

Smith-Vidaurre, G., Araya-Salas, M., & Wright, T.F. (2020). Individual signatures outweigh social group identity in contact calls of a communally nesting parrot. *Behavioral Ecology*, *31*(2), 448–458. https://doi.org/10.1093/beheco/arz202

Smith-Vidaurre, G., Perez-Marrufo, V., Hellmich, D. L., Hobson, E.A., Salinas-Melgoza, A. & Wright, T.F. (2021). *Hierarchical mapping patterns persist in learned calls of a parrot following invasion*.

Manuscript in preparation.

Sol, D., Santos, D.M., Feria, E., Clavell, J., & Feria, E. (1997). Habitat selection by the monk parakeet during colonization of a new area in Spain. *Condor*, *99*, 39–46.

Thielcke, G. (1973). On the origin of divergence of learned signals (songs) in isolated populations. *Ibis*, *115*(4), 511–516. https://doi.org/10.1111/j.1474-919X.1973.tb01989.x

Tibbetts, E.A., & Dale, J. (2007). Individual recognition: It is good to be different. *Trends in Ecology & Evolution*, *22*(10), 529–537. https://doi.org/10.1016/j.tree.2007.09.001

Tibbetts, E.A., Liu, M., Laub, E.C., & Shen, S.F. (2020). Complex signals alter recognition accuracy and conspecific acceptance thresholds. *Philosophical Transactions of the Royal Society B: Biological Sciences*, *375*(1802), 20190482. https://doi.org/10.1098/rstb.2019.0482

Valletta, J.J., Torney, C., Kings, M., Thornton, A., & Madden, J. (2017). Applications of machine learning in animal behaviour studies. *Animal Behaviour*, *124*, 203–220. https://doi.org/10.1016/j.anbehav.2016.12.005

Van Bael, S., & Pruett-Jones, S. (1996). Exponential population growth of monk parakeets in the United States. *Wilson Bulletin*, *108*(3), 584–588.

Venables, W.N., & Ripley, B.D. (2002). *Modern applied statistics with S* (4th ed.). New York, NY: Springer.

Volpe, N.L., & Aramburu, R.M. (2011). Preferencias de nidificacion de la cotorra argentina (*Myiopsitta monachus*) en un area urbana de Argentina. *Ornitologia Neotropical*, *22*, 111–119.

Wanker, R., Sugama, Y., & Prinage, S. (2005). Vocal labelling of family members in spectacled parrotlets, *Forpus conspicillatus*. *Animal Behaviour*, *70*(1), 111–118. https://doi.org/10.1016/j.anbehav.2004.09.022

Wickham, H. (2016). *ggplot2: Elegant graphics for data analysis*. New York, NY: Springer-Verlag.

Wright, M.N., & Ziegler, A. (2017). ranger: A fast implementation of random forests for high dimensional data in C++ and R. *Journal of Statistical Software*, *77*(1), 1–17. https://doi.org/10.18637/jss.v077.i01

Appendix

Proxies of Local Population Size and Maximum Social Group Size per Range

Nest variables and flock sizes per range

Total estimated nests at nesting sites, nesting site areas and nest densities were obtained as described in the main text. Nesting sites (at which nest observations were made and recording sessions were performed) are hereafter referred to as 'sites' in all subsequent sections. For Mann–Whitney–Wilcoxon tests, repeated observations at sites (sites visited over more than one year) were removed to meet assumptions of independent samples. Four invasive range observations of estimated total nests were dropped that represented sampling of the same sites over two years (sites AIRP, ELEM, INTR, MART in 2011 were dropped, see Table A4 for full site names). For site areas and nest densities, two invasive range observations were dropped that represented sampling of the same sites in different years (sites INTR and MART in 2011 were dropped). Mann–Whitney–Wilcoxon tests were carried out with the package coin v.1.3-1. Maximum flock sizes were obtained as described in the main text, employing observations from field notebooks, and statistical testing was performed with Mann–Whitney–Wilcoxon tests as described in the main text. These comparisons of total estimated nests, site areas and nest densities were largely performed between native range agro-interface sites and invasive range urban sites, although one native range site in the city of Montevideo (Bodegas Carrau) was considered urban (see below, Validating the Effect of Urban and Agro-interface Habitats between Ranges; Table A2). See the script 'SimplerSignatures_AdditionalMaterials_01_SummaryStatistics_ NestVariables_SocialGroups.Rmd' and the knitted RMarkdown output provided on GitHub for more information.

Pest control and proxies of local population size

Monk parakeets have been considered agricultural pests in their native range since the 1800s (Russello, Avery, & Wright, 2008). Methods employed during attempts to reduce population sizes in the native

range include poisoning and burning nests (Eberhard, 1998) as well as lopping off the tops of tall trees in which the parakeets nest (which has the effect of removing original nests but also making subsequent nests more accessible for control efforts once rebuilt). Native range parakeets in Uruguay were observed to rebuild quickly after attempts to control populations, in either the same trees or trees nearby. In this study, at sites INIA Las Brujas (INBR) and el Centro de Entrenamiento Hípico Punta del Este (HIPE), nests had been rebuilt in eucalyptus trees with the tops lopped off. At INBR, nests had been rebuilt within a month of control efforts, and evidence of a poisoning treatment with the insecticide carbofuran was also observed (G. Smith-Vidaurre, personal observation).

In the invasive range, nests are often removed by electrical utility companies (Avery, Tillman, Keacher, Arnett, & Lundy, 2012), and it does seem that parakeets also rebuild nests in response to this form of disturbance, consistent with previous reports (Burgio, van Rees, Block, Pyle, Patten, et al., 2020). An example in our study was the University of Texas – Austin Intramural Fields (INTR), at which 20 nests were observed in 2011 in stadium lights, and in 2019, nests were no longer observed in stadium lights (likely due to nest removal), but rather 13 nests were found in trees and telephone poles adjacent to the Intramural Fields (Table A2). This site displayed the greatest numbers of nests observed for any invasive range site we surveyed, despite such likely pest control measures. As pest control is undertaken in each range, but parakeets rebuild nests following such disturbance, the difference in the total estimated nests and nest densities we reported in this work was unlikely to be driven by pest control activities.

Influence of habitat on the social environment

Differences in habitat should have more of an effect on population contiguity and opportunities for social interactions in this system rather than the number of nests at a given site. Monk parakeets build communal and colonial nests on various substrates using sticks obtained from vegetation near nests (Avery et al., 2012; Burgio et al., 2020; Pranty, 2009; Sol, Santos, Feria, Clavell, & Feria, 1997; Volpe & Aramburu, 2011). Nests are often located inside or near green spaces that provide sufficient vegetation for nest building, and

parakeets often forage at their nesting sites (Sol et al., 1997; G. Smith-Vidaurre, personal observation), which ties this species to green spaces regardless of habitat type. Urban green spaces can be more geographically distant from each other compared to nonurban habitats due to habitat fragmentation (Goddard, Dougill, & Benton, 2010); therefore, urban parakeets should experience fewer opportunities for social interactions among nesting sites, limiting social group sizes in urban habitats. Nests are used for roosting throughout the year and comprise the foci of most social interactions (Burgio et al., 2020; Sol et al., 1997). As such, most social interactions and related acoustic signalling should largely take place in or near green spaces characterized by less low-frequency anthropogenic noise. In our own fieldwork, we observed urban parakeets in both ranges exploiting fragmented green spaces (G. Smith-Vidaurre, personal observation).

The variation in natural and artificial nest substrates that parakeets used in both the native and invasive ranges was consistent with previous reports (Avery et al., 2012; Pranty, 2009; Sol et al., 1997; Volpe & Aramburu, 2011), indicating that parakeets are not limited in nest building by the availability of substrates in different habitats. Parakeets use green spaces with trees in which nests can be built and which also provide sticks for nest building. In Uruguay and the United States, we observed parakeets building on a wide variety of nest structures, including electrical transformers, pylons and various native and exotic trees in different habitats, which was an indication that in the populations we studied, differences in habitat between ranges did not place significant limitations on the availability of resources for nest building. Instead, it is more likely that the total number of individuals present in local populations was the limiting factor for the differences in estimated total nests and nest densities that we identified in each range.

Contact Call Recording and Prepreprocessing

Recording contact calls

Recordings were made using recording rigs, sampling rates and bit depths detailed in the main manuscript. Recordings were made onto a single channel. The 2004 calls provided as cuts of original recordings

were previously high-pass filtered at 600 Hz to remove low-frequency noise in the background (Buhrman-Deever, Rappaport, & Bradbury, 2007). Contact calls were recorded similarly across ranges and years, and were generally obtained from unmarked parakeets flying in or out of clusters of nests, as well as perched individuals (Buhrman-Deever et al., 2007; Smith-Vidaurre, Araya-Salas, & Wright, 2020). We obtained a single call per unmarked bird (Tables A3, A4), with the exception of a subset of repeatedly sampled individuals (Table A5). These repeatedly sampled individuals (3 marked native range individuals, 5 unmarked native range individuals, and 9 unmarked invasive range individuals) were recorded perched alone while performing short bouts of calling, or were isolated using narrations made during recording sessions, as described in Smith-Vidaurre et al. (2020). These two data sets (one call per unmarked individual versus various calls from repeatedly sampled individuals) yielded broad geographical sampling and depth of individual sampling, respectively, that we employed for analyses as described in the main text.

Native range sites were recorded from May through to November 2017, which overlapped with the beginning of native range monk parakeets' breeding season, documented to begin in October or November in populations in northern Argentina (Eberhard, 1998). This is a region close to Uruguay, where native range populations were sampled for the present study. Invasive range recordings in 2004 were made in March and April (Buhrman-Deever et al., 2007), while 2011 recordings were made in February, 2018 recordings were made in April and 2019 recordings were made in August. In invasive populations in Florida, monk parakeet breeding has been documented to begin in March, with fledglings emerging prior to August (Avery et al., 2012). As such, invasive range recordings were likely performed at the beginning or end of the breeding season in different years.

Call selection in Raven and preprocessing calls in R

Contact calls were manually selected in Raven v.1.5 (Cornell Lab of Ornithology Bioacoustics Research Program, 2014) from 2017 native range recordings in previous work (Smith-Vidaurre et al., 2020). Calls were selected from 2011, 2018 and 2019 invasive range recordings with Raven v.1.4 (Cornell Lab of

Ornithology Bioacoustics Research Program, 2014). Previously published 2004 contact calls were provided as cuts of original recordings (Buhrman-Deever et al., 2007) and were downsampled to 44.1 kHz. Unless specified otherwise, call prepreprocessing was performed in R v.3.4.4 (R Core Team, 2018) with the warbleR package v.1.1.18 (Araya-Salas & Smith-Vidaurre, 2017). Invasive range calls, including 2004 calls, were taken through a similar preprocessing workflow (Buhrman-Deever et al., 2007; Smith-Vidaurre et al., 2020). We made catalogues of invasive range calls and visually checked call quality. Calls were assigned a score of low, medium or high visual quality. We also checked for visible patterns of amplitude saturation, overlapping signals in the background and visible truncation of calls (2004 cuts), and added this metadata to a spreadsheet for manually detected calls. We used this metadata to retain high-quality calls. Calls with low-quality scores, visible amplitude saturation, overlapping signals or signal-to-noise ratio less than 7 were dropped, as in Smith-Vidaurre et al. (2020).

Temporal coordinates of calls were tailored by the same observer to return consistent start and end times across the native and invasive range data sets. Spectrograms were generated for individual calls to visually validate call quality and consistency of temporal coordinates, using the following settings: Hanning window, window length of 378, window overlap of 90. Unless otherwise specified, we used the same settings for all measurements below relying on Fourier transformations and spectral measurements (e.g. spectrographic cross-correlation), in addition to a band-pass filter of 0.5–9 kHz. We combined extended selection tables for the native and invasive ranges and filtered the resulting selection table to retain sites with at least five calls after preprocessing (Tables A3, A4) as well as known repeatedly sampled individuals with four or more calls (Table A5). Extended selection tables are a file structure in R supported by the warbleR package (Araya-Salas et al., 2017) that combine temporal coordinates of selected vocalizations with metadata and the .wav files of the selected calls themselves.

We dropped duplicate recording sessions when a site was re-recorded on different days. However, some sites in the current data set were represented by calls recorded on different days. This was due to merging sites that represented very fine-scale geographical sampling, which had been used for previous comparisons of

geographical variation in the native range (Table A3) (Smith-Vidaurre et al., 2020). Also, for a complementary study, we included one call per repeatedly sampled individual in the larger data set of a single call per individual, which led to more than one recording date for some sites with known repeatedly sampled individuals. The full data set contained 1596 calls across the two abovementioned data sets and ranges. Summary statistics for these two data sets are described in more detail in the main text. For supervised machine learning analyses below, we dropped the single call per each known repeatedly sampled individual included in the larger data set to avoid including duplicated calls, yielding a total of 1561 calls. See the script 'SimplerSignatures_AdditionalMaterials_01_SummaryStatistics _NestVariables_SocialGroups.Rmd' and the RMarkdown output provided on GitHub for more information.

Assessing General Differences in Acoustic Structure between Ranges with Supervised Machine Learning

Obtaining predictors for machine learning

We obtained a large set of acoustic measurements, including a standard set of 27 spectral acoustic measurements: duration, mean frequency, standard deviation of frequency, median frequency, first quartile frequency, third quartile frequency, frequency interquartile range, median time, first quartile time, third quartile time, time interquartile range, skew, kurtosis, spectral entropy, time entropy, spectrographic entropy, spectral flatness, mean dominant frequency, minimum dominant frequency, maximum dominant frequency, dominant frequency range, modulation index, start dominant frequency, end dominant frequency, dominant frequency slope, mean peak frequency and peak frequency (Araya-Salas et al., 2017). Modulation index was measured using the dominant frequency time series, and therefore represented a single index of the degree of modulation of the dominant frequency per call. In addition, 88 descriptive statistics were obtained for 12 total Mel-frequency cepstral coefficients (MFCC) calculated with 40 warped spectral bands, as additional measurements that described variation in contact call structure. These statistics included the mean, median, minimum, maximum,

kurtosis, skewness and variance of each cepstral coefficient as well as the mean and variance of the first and second derivatives (Araya-Salas et al., 2017).

We also measured acoustic similarity of calls to obtain patterns of acoustic variation present in the data set that could be useful for supervised machine learning. Acoustic similarity was measured using spectrographic cross-correlation (SPCC) on spectrograms and Mel-frequency cepstral coefficients, dynamic time warping (DTW) on spectral entropy and dominant frequency time series estimated at 100 time points per call and multivariate DTW (multiDTW) on spectral entropy and dominant frequency time series. These acoustic and similarity measurements were calculated with warbleR v.1.1.18 in R v.3.4.4. Acoustic measurements were converted to features for supervised machine learning using principal components analysis (PCA) and similarity measurements were converted to features via multidimensional scaling (MDS). Prior to performing PCA, acoustic measurements were preprocessed using a Yeo–Johnson transformation, centering and scaling, and removing zero variance and near zero variance variables. MDS was performed with 15 dimensions per similarity method and 1000 maximum iterations to find an optimal solution. Converting raw measurements to features yielded new predictors that represented variation across calls while reducing collinearity present among the original raw measurements.

We filtered out calls that were used for a complementary study, yielding 1561 calls for supervised machine learning analyses (see above, Call selection in Raven and preprocessing calls in R), then combined features extracted with MDS and PCA with the 27 standard spectral acoustic measurements described above to yield 217 predictors. This set of predictors was filtered for high collinearity using Pearson's correlation (predictors with Pearson's r less than or equal to 0.75 were retained). We did not identify predictors that exhibited a high Pearson's correlation with signal-to-noise ratio measurements. After dropping highly collinear predictors, we obtained a final set of 203 predictors for machine learning, which included 15 standard spectral acoustic measurements (see below) and 188 features derived by MDS and PCA.

The following 15 standard acoustic measurements were retained: start and end dominant frequency, minimum and maximum dominant frequency, dominant frequency range and slope, modulation

index, peak frequency, mean peak frequency, frequency interquartile range, third frequency quartile, kurtosis, spectral entropy, duration and first temporal quartile. These acoustic measurements were used as predictors so as to directly evaluate their importance for the classification of calls back to ranges, as it is easier to attribute structural differentiation to original measurements (such as call duration) rather than features representing less interpretable combinations of original measurements (e.g. principal components). The remaining 188 predictors were composed of 75 MDS and 113 PCA features: 15 MDS features from each the five similarity measurements employed (SPCC on spectrograms, SPCC on MFCC, DTW on dominant frequency time series, DTW on spectral entropy time series, multivariate DTW (on dominant frequency and spectral entropy time series)), 25 features derived by PCA on the 27 standard acoustic parameters and 88 features derived by PCA on MFCC.

Splitting calls for machine learning

We split the data set of 1561 calls into training, validation and prediction data sets in R v.3.6.3. All subsequent analyses were performed with this version of R. Calls per site were randomly split depending on whether or not a site was used for spatial (between ranges) or temporal (among years in the invasive range) comparisons of acoustic structure. For native range sites and each invasive range site that did not represent temporal sampling, we randomly sampled one-half of the total calls for training. Among the remaining calls per site, we randomly sampled one-third of the calls for validation and set aside the remaining two-thirds of the calls for prediction. For invasive range sites that did represent temporal sampling (e.g. the same site sampled in different years, or sites representing a city sampled over years, which applied to only Austin, Texas and New Orleans, Louisiana sites), we randomly sampled 20 calls for prediction. If one of these sites had 20 calls or less, we took all calls for prediction. For temporally sampled sites with more than 20 calls, we randomly chose one-half of the remaining calls for training and set aside the other half for validation. All random sampling was performed without replacement.

This overall sampling scheme yielded 676 calls for training, 337 calls for validation and 548 calls for prediction, while sampling as evenly as possible from different spatial regions and years in the invasive range

data set. Training, validation and prediction data sets contained 43%, 22% and 35%, respectively, of the 1561 calls used for supervised machine learning. The prediction data set contained invasive range calls from all areas sampled in the U.S. for our direct comparison between ranges and also contained invasive range calls sampled over time in Austin and New Orleans to assess the possibility of structural change in invasive range calls over time.

Model training, validation and prediction

Supervised stochastic gradient boosting and random forests models were built to classify calls back to either the native or invasive range. Models were trained and tuned with the 203 predictors described above over five iterations of repeated five-fold cross-validation using caret v.6.0-86 (Kuhn, 2020), gbm v.2.1.5 (Greenwell, Boehmke, Cunningham, & GBM-Developers, 2019) and ranger v.0.12.1 (Wright & Ziegler, 2017). The total number of trees, interaction depth (maximum depth of each tree, or the highest level of interactions permitted among predictors) and shrinkage parameter (learning rate of the model) were tuned for the gradient boosting model. The mtry parameter (the number of predictors randomly selected at each split) was tuned for the random forests model. After evaluating training performance, we visualized variable importance per model. Although the random forests model had slightly lower training classification accuracy, it exhibited more of the standard spectral acoustic measurements among the top 30 most important variables for classification back to ranges. As we wanted to use these spectral acoustic measurements to more closely evaluate structural differences between ranges, we selected the random forests model for validation and prediction. This model yielded high validation accuracy, so we proceeded with prediction, and found that the model demonstrated high prediction accuracy back to ranges (Table A6).

Finer-scale assessment of structural change

High classification accuracy during model training, validation and prediction indicated high structural differentiation between ranges. These structural differences were visualized by reducing the random

forests proximity matrix to two dimensions with MDS. Density in acoustic space per range was obtained by applying a two-dimensional Gaussian kernel density estimator with bandwidth of 0.5 in each dimension to the MDS coordinates. Contours were generated by splitting density values into 10 bins, such that each contour delineated 1/10th of the total density per range (Fig. 2b). The visualization was made with the ggplot2 package (v.3.3.3) (Wickham, 2016), which relies on the package MASS (v.7.3-51.6) (Venables & Ripley, 2002) for the two-dimensional kernel density estimator. Finer-scale spatial and temporal structural changes were evaluated by assessing classification accuracy for calls set aside for spatial and temporal comparisons in the random forests prediction data set, using misclassification back to the native range as an indicator of structural change (e.g. invasive range calls becoming more native range-like, or vice versa).

We expected that, if invasive range populations grew in size over time, then these populations should experience greater selection for more distinctive individual signatures, and therefore, invasive range calls could become more structurally similar to native range calls over time. If so, we expected to see higher misclassification of invasive range calls over time, or in different sampling areas that may have exhibited larger population sizes but were not sampled over time. However, we found no clear changes in classification accuracy over regions or years in the invasive range, which indicated that structural differences identified between ranges largely held regardless of the year and region in which invasive populations were sampled (see code provided on GitHub: http://github.com/gsvidaurre/simpler-signatures-post-invasion). We also validated misclassification of invasive range calls and found that misclassification was not due to low signal-to-noise ratio (e.g. misclassified calls were not lower-quality calls). Finally, structural changes in calls between ranges were assessed at a finer structural scale by assessing partial dependency of random forests classification accuracy on the 15 original acoustic measurements used among predictors. Partial dependency plots showed little change in classification accuracy back to the invasive range, indicating that structural differences between ranges did not entirely map onto these 15 standard acoustic measurements. See the script 'SimplerSignatures_AdditionalMaterials_02_ AcousticStructure_SupervisedML.Rmd' and the knitted RMarkdown output provided on GitHub for more information.

Obtaining Frequency Modulation Measurements

Comparisons of frequency modulation patterns and individual identity content

Calls were subsampled for frequency tracing, as we relied on manual tracing and this would have been prohibitively time-consuming to perform for the entire data set. We randomly selected a subset of calls from the large data set of a single call per individual (e.g. not the data set of known repeatedly sampled individuals) for a spatial comparison between the native and invasive ranges, as well as calls for a temporal comparison within the invasive range. We used temporal comparisons to account for the possibility of temporal change in acoustic structure, which could confound direct comparisons between ranges. Ten sites were randomly selected per range, and four calls were randomly chosen per site. Overall, 80 calls were selected to evaluate frequency modulation patterns between ranges. These calls represented all sampling regions in the native range relatively evenly, although Texas was more heavily represented in the invasive range calls, as the full data set contained more calls from this area.

For temporal comparisons of frequency modulation, we chose 15 site-years from Austin and New Orleans that represented sampling over time. Austin sites were each sampled in two years (10 site-years total, sampled in either 2011 and 2019, 2004 and 2019, or 2004 and 2011), while the same New Orleans sites were not sampled over different years, but together represented temporal sampling at the city scale (3 sites sampled in 2004, 2 sites sampled in 2011). We randomly selected five calls per each site-year, yielding a total of 75 invasive range calls for temporal comparisons. Twenty-five calls were selected for 2004 (Austin and New Orleans), 30 calls were selected for 2011 (Austin and New Orleans) and 20 calls were selected for 2019 (Austin only).

We also randomly sampled five calls per repeatedly sampled individual per range, or took all calls for repeatedly sampled individuals with five or fewer calls, yielding a total of 84 calls that were tapped for analyses of individual identity content present in frequency contours that encoded individual signatures (see below, Assessing Individual Identity Content). Our overall sampling scheme for frequency tracing yielded 239

calls total, with six calls randomly sampled from 3 site-years for both the spatial and temporal comparisons (1 call from BALL-2004 in New Orleans, 1 call from INTR-2011 in Austin, 4 calls from VALL-2004 in Austin), so we performed frequency tracing for 233 calls total.

Tracing second harmonic frequency contours

Frequency contours were obtained by estimating fundamental frequency as a time series at 100 time points per call, and these contours were used to manually trace the second harmonic per call with warbleR v.1.1.24. Unless otherwise specified, we used this version of warbleR for all subsequent analyses. We chose to trace the second harmonic because the fundamental frequency was not estimated accurately with respect to harmonics visible in monk parakeet contact calls, and the fundamental frequency contour was also not always clearly visible across calls. The subset of calls selected above for frequency tracing was randomly split in half to spread the manual-tracing workload across two observers. Tailored contours per observer were then combined and a final round of tailoring was performed by one observer. Finally, spectrograms of calls with frequency contours were generated and inspected as a final check of tracing accuracy.

Estimating peaks and troughs of frequency contours

To measure frequency modulation patterns, we dropped five points from the start and end of each contour to account for small gaps preceding or following calls, and some end points that fell underneath components of the graphical user interface used for tailoring. We then randomly selected five calls per range from the subset of calls with frequency contours and generated image files of the frequency contours. One observer manually counted large, visible frequency peaks and troughs per call. This step was performed in order to inform our automated approach for estimating peaks and troughs (inverted peaks). Once we obtained the number of visible peaks and troughs per call, we applied a general peak-locating function to frequency contours of the randomly sampled set of 10 calls above, using pracma v.2.2.9 (Borchers, 2019). This initial peak search

was used to fine-tune a more automated custom peak and trough estimation routine across the 233 calls with frequency contours.

From the preliminary peak search above, we obtained the maximum peak height identified in the subset of 10 calls and used this to implement a threshold on minimum peak height in the customized function below. We also implemented smoothed spline interpolation of frequency contours, using the built-in R package stats v.3.6.3. Spline interpolation was performed with an exact cubic spline over five times the length of each manually traced frequency contour (e.g. 90 points were interpolated to yield 450 points), with means obtained for tied values. Cubic smoothing splines were applied to the interpolated points, and we optimized degrees of freedom, a parameter that controlled the degree of smoothing. Spline interpolation and smoothing helped flatten small peaks introduced by manual tailoring. The pracma package was used as above to estimate frequency peaks of the smoothed spline-interpolated points. Limitations were imposed on the peaks identified by pracma: peaks could not be within two points of the end of the smoothed frequency contour; peaks had to exhibit heights greater than a minimum height threshold (obtained above) compared to preceding frequency points; peaks had to be a minimum distance apart (to filter out multiple peaks identified when a single tall peak presented as a plateau). We estimated troughs by searching for peaks across the inverted smoothed contours with pracma. Once troughs were obtained, we assigned them to closest preceding peaks and removed troughs that were not assigned to peaks. This routine returned peaks and troughs per call, as well as the slope per peak–trough pair (change in frequency/change in indices of smoothed contours), and image files for visual inspection of results.

We applied this customized function to the 233 calls with frequency contours and visually inspected the peaks and troughs estimated per call to settle on final parameters for the function. Overall, the customized peak–trough estimation routine performed well when estimating large frequency peaks and identifying troughs following each large peak. In a few cases, medium or small frequency peaks close to large peaks were not identified, and in other cases, gradual increases in frequency were labelled as peaks (and sometimes were not assigned troughs). Missing peaks per call could lead to underestimation of frequency modulation measurements. However, we felt this would not bias our results because peaks were missed for only

a few calls in the data set, and when this did occur, only a single peak was missed per call. In addition, the peaks missed were of small/medium height and not representative of large changes in frequency modulation. On the other hand, visual inspection indicated that overestimation of frequency modulation was more of a problem (very small peaks or gradual rises in frequency identified as peaks). We addressed this concern by (1) removing peaks per call that were not matched to troughs and (2) binning peak–trough slopes into 50 classes and removing peaks in the last two bins, which represented very small or positive peak–trough slopes. After dropping 170 peaks in these two bins, we proceeded with frequency modulation measurements across the 233 calls.

Calculating frequency modulation measurements

Frequency modulation patterns were assessed by obtaining three customized frequency modulation measurements: the total number of peaks, the modulation rate (number of peaks/call duration) and the maximum peak–trough slope (largest negative slope between a given peak and neighbouring trough) per call. These frequency modulation measurements were not captured by other acoustic measurements obtained in this work. The modulation rate measurement was not equivalent to the modulation index calculated above (see above, Obtaining predictors for machine learning), as modulation rate was calculated based on the manually traced second harmonic frequency contours, while the modulation index measurement represented modulation of the dominant frequency. In monk parakeet calls, the dominant frequency naturally changes among harmonics; therefore, the modulation rate and the modulation index captured different aspects of frequency modulation in these signals. We obtained medians and interquartile ranges (IQR) for each frequency modulation measurement per range, as well as for the 27 standard spectral acoustic measurements that were previously used for machine learning (see above, Obtaining predictors for machine learning), with the set of 80 subsampled calls as described above. The effect size of range was calculated as Cliff's delta (Cliff, 1996) with bootstrapped 95% confidence intervals (CIs) for each of the 30 total acoustic measurements (3 customized frequency modulation measurements, 27 standard spectral acoustic measurements) using the orddom package v.3.1. Cliff's delta was employed to calculate effect sizes robust to the non-normality and heterogeneous variance we identified in our

data (Hess & Kromrey, 2004). We used a rule-of-thumb to identify large effect sizes, such that absolute effect sizes greater than or equal to 0.474 were considered large (Romano, Kromrey, Coraggio, Skowronek, & Devine, 2006) and treated effect sizes as statistically significant when 95% CIs did not include zero (Table A7).

We accounted for the possibility of temporal change in acoustic structure for the invasive range by evaluating the overall distributions of six acoustic measurements for the data set of 75 calls selected for temporal comparisons. These six measurements were chosen because these same measurements had displayed the largest effect sizes in the comparison above between ranges. There was little visible change over time in these six acoustic measurements in the invasive range, indicating that the structural differentiation we identified between ranges was consistent over sampling intervals in the U.S. that spanned 15 years (Fig. A1). See the script 'SimplerSignatures_AdditionalMaterials_03_ AcousticStructure_FrequencyModulation_HabitatAnalyses.Rmd' and the knitted RMarkdown output provided on GitHub for more information.

Assessing Individual Identity Content

Validation analysis of individuals used to calculate Beecher's statistic

We used Beecher's statistic to calculate the amount of individual identity content in calls of repeatedly sampled individuals per range (Beecher, 1989; Linhart, Osiejuk, Budka, Salek, Spinka, et al., 2019). Here, we felt it was important to use equal numbers of individuals that represented similar patterns of variation in acoustic space per range. Previous work indicated that individuals at the same site, as well as sites separated by short geographical distances, are overdispersed in acoustic space, but individuals begin to overlap in acoustic space over increasing geographical distances (Smith-Vidaurre et al., 2020). In our data set of repeatedly sampled individuals, the three native range sites at which we repeatedly sampled individuals were separated by greater distances (minimum distance of 11.12km apart) than the three sites sampled for the invasive range (3.44–7.45 km apart), which we felt could influence Beecher's statistic if native range individuals separated by greater

geographical distances overlapped more in acoustic space. Therefore, we identified five repeatedly sampled individuals that represented restricted geographical areas per range, recorded at either a single site-year in the native range (site 1145 in 2017), or recorded at three sites in single year (city of Austin in 2019) in the invasive range. As we had not obtained repeated calls for five individuals at a single invasive range site, we performed a validation analysis to ask whether these two sets of individuals indeed represented similar patterns of call variation per range.

A resampling analysis was designed to evaluate patterns of variation in second harmonic frequency contours represented by three sets of individuals: the five native range individuals randomly sampled from three sites, the five native range individuals recorded at a single site (site 1145) and the five invasive range individuals recorded at three sites in Austin 2019. DTW was performed on second harmonic frequency contours (no spline interpolation or smoothing, and five points were dropped from the start and end of each contour) to obtain pairwise acoustic distances. Per resampling iteration, we randomly sampled four calls per individual without replacement (or took all calls if there were only 4 total). For the native range comparison with three sites, we randomly sampled five of the eight total individuals recorded over three sites without replacement. Then per individual, we obtained the difference in mean DTW distance within each individual compared to other individuals for the given range and comparison. This resampling process was repeated over 1000 iterations. The mean difference in DTW distance and 95% CIs were calculated per range and comparison. Mean DTW differences were similar between the five native range individuals from a single site and the five invasive range individuals at three sites, but were lower for five individuals randomly sampled from three native range sites over resampling iterations (Fig. A2). Therefore, the individuals from the three native range sites (representing greater geographical spread than the invasive range individuals) were more likely to overlap in acoustic space. The native range individuals from a single site and the invasive range individuals from three sites did indeed represent similar patterns of acoustic variation, so we proceeded with these individuals for Beecher's statistic calculations.

Calculation of Beecher's statistic

Beecher's statistic (HS) was calculated through the IDmeasurer package v.1.0.0 (Linhart et al., 2019) and R version 4.1.0 using two acoustic measurements: 88 descriptive statistics of MFCC and second harmonic frequency contours. For each measurement, we used the five calls sampled for tracing frequency contours for five individuals per range. These five calls were randomly sampled for each individual, or represented the total number of calls if only five calls were recorded for a given individual. As in frequency modulation analyses above, five points were dropped on either end of each frequency contour, but we did not perform spline interpolation or smoothing. HS was reported using the sum of principal components significantly related to individual identity (e.g. significantly different among individuals) (Table 1). We estimated the number of potential unique individual signatures per range and measurement as 2^{HS} (Table 1) (Beecher, 1989; Linhart et al., 2019). See the script 'SimplerSignatures_AdditionalMaterials_04 _IdentityContent.Rmd' and the knitted RMarkdown output provided on GitHub for more information.

Validating the Effect of Urban and Agro-interface Habitats between Ranges

During our fieldwork in Uruguay, we observed native range monk parakeets nesting and foraging in nonurban areas characterized by various agricultural activities, including cattle grazing and seasonal crop farming, which we considered 'agro-interface' habitats. However, monk parakeets have also invaded cities in their native range. In Uruguay, the capital city of Montevideo is the largest urban area and likely poses the only true urban habitat for monk parakeets in this country, as other cities are small enough for monk parakeets to fly beyond city limits for foraging, as observed in the city of Colonia del Sacramento on the west coast. We recorded at four sites in Montevideo that we considered urban sites: Bodegas Carrau (BCAR, a vineyard on the edge of Montevideo next to a busy road), la Facultad de Agronomía (FAGR, a satellite campus of la Universidad de la República with many trees and gardens), el Cementerio Central (CEME, a green space in the middle of Montevideo, far from agricultural areas) and el Club de Golf (GOLF, a green space also far from agricultural

areas). Monk parakeets living in Montevideo were observed exploiting the green spaces scattered throughout the city for nesting as well as foraging.

Invasive range parakeets were largely recorded in cities, in line with previous work that has documented that U.S. invasive range populations are often restricted to urban areas, at least in the northern part of the country (Davis, Malas, & Minor, 2014). Our field observations in 2011 and 2019 indicated that monk parakeets also exploited green spaces in cities in the U.S. for either nesting and/or foraging. Thirty-three out of the 37 total native range sites used in this study were found in agro-interface habitats (Table A3), while we considered all invasive range sites as urban. As such, our comparison between ranges also contained a partially confounded comparison between habitat types. Here, we took advantage of calls recorded at these four native range urban sites to determine whether urban habitats could explain some of the changes in acoustic structure we reported between ranges.

Random forests misclassification by native range habitat

During random forests prediction, we used a subsample of randomly selected calls from each of the aforementioned native range urban sites. We assessed misclassification of these native range urban calls, as classification back to the invasive range would indicate that such native range urban calls were more similar to invasive range calls recorded in similar habitats (similar to previous assessments of call misclassification; see above, Finer-scale assessment of structural change). Twenty-four out of 230 native range calls were misclassified during random forests prediction, and of these calls, only two represented native range urban sites (1 out of 5 calls misclassified for BCAR, 1 of 2 calls misclassified for FAGR). Ten native range agro-interface sites displayed anywhere from one to six calls each that were misclassified as invasive range calls. These results indicated that when using a large set of acoustic features to capture overall patterns of acoustic variation, there was low support for structural differences among calls recorded in different habitats in the native range. However, few native range urban calls were included in the prediction data set, which could underlie the lack of identification of differences among habitats by supervised machine learning.

Visualizing separation by habitat and range through PCA on spectral acoustic measurements

We visualized separation among calls recorded in the three distinct range–habitats represented in this study (native range agro-interface, native range urban, invasive range urban) using PCA on 27 standard spectral acoustic measurements obtained with the warbleR package (Araya-Salas et al., 2017). This analysis had already been performed to obtain features for random forests analysis (see above, Obtaining predictors for machine learning). Four sites were chosen per habitat type for PCA visualizations. For native range agro-interface sites, we used four sites recorded in the department of Colonia, Uruguay in 2017 (Piedra de los Indios (PIED), INIA La Estanzuela 08 (INES-08), Las Leñas (LENA), INIA La Estanzuela 03 (INES-03)). Native range urban sites were represented by the four aforementioned sites above. For invasive range sites (also considered urban), we used sites César Chavez Fields (SOCC), Sam L. Martin Middle School (MART), University of Texas-Austin Intramural Fields (INTR) and the University of Texas-Austin Elementary School (ELEM), all recorded in Austin, Texas, in 2019. As the four invasive range sites each had about twice as many calls as the native range sites in either habitat category, 20 calls were randomly selected without replacement for each invasive range site used. This data set contained 82, 48 and 80 total calls for the native range agro-interface, native range urban and invasive range urban habitat categories, respectively.

Calls were visualized in low-dimensional acoustic space by filtering the PCA results (obtained for the larger data set of calls used for supervised machine learning; see above, Obtaining predictors for machine learning) by the calls selected for habitat analyses and plotting the first two principal components (PCs). These previous PCA results were employed to evaluate habitat differences within the same acoustic space that represented the larger data set of calls. The original acoustic measurements with the five highest loadings onto PC1 were entropy, spectral flatness, spectral entropy, standard deviation of frequency and frequency interquartile range (all negative loadings). Measurements with the five highest loadings onto PC2 were mean frequency, median frequency, mean dominant frequency, first quartile frequency and third quartile frequency (all negative loadings as well). Together, PC1 and PC2 explained 44.3% of the variation in the full data set of calls used for

machine learning. Calls across range–habitats were visualized in low-dimensional acoustic space by employing a two-dimensional Gaussian kernel density estimator in a similar manner as for random forests acoustic space above, although with a bandwidth of 5 (see above, Finer-scale assessment of structural change), such that the resulting density contours represented bins of 1/10th of the density of calls per range–habitat in acoustic space (Fig. A3).

Effects of habitat and range on acoustic measurements

As the visualization of calls in low-dimensional acoustic space indicated there were differences by habitat in the native range (Fig. A3), we assessed the independent effects of habitat and range on the 27 spectral acoustic measurements for the data set of calls used for habitat analyses, as well as the three customized frequency modulation measurements used in this study that were obtained with a smaller subsample of calls. To assess the effect of habitat on acoustic structure, we used the 82 native range urban and 48 native range agro-interface calls (e.g. comparing between habitats within the native range) to obtain the effect size of habitat on the 27 acoustic measurements. To evaluate the effect of range on acoustic structure, we used the 48 native range urban and 80 invasive range urban calls (e.g. comparing within urban habitat and between ranges) to calculate the effect size of range on the 27 acoustic measurements. Effect sizes were obtained as Cliff's delta with bootstrapped 95% CIs (Table A8).

Effect sizes of range and habitat were also obtained for frequency modulation measurements calculated with second harmonic frequency contours (number of peaks, modulation rate, peak–trough slope; see above, Calculating frequency modulation measurements). For these effect sizes, we used calls subsampled for frequency modulation measurements. For the native range agro-interface and urban calls, we used eight calls from sites La Piedra de los Indios (PIED) and INIA La Estanzuela – 08 (INES-08) and eights calls from sites La Facultad de Agronomía (FAGR) and El Club de Golf de Montevideo (GOLF), respectively, all recorded in 2017. For the invasive range urban calls, we used eight calls from sites Airport Boulevard (AIRP) and Manor Rd (MANO), recorded in Austin in 2019. In summary, we used four calls each from two sites in each range–habitat

category (6 sites and 24 calls total). Although these sample sizes were small, using calls employed for the comparison of frequency modulation patterns between ranges above (see above, Calculating frequency modulation measurements) allowed us to assess whether the effect of range on frequency modulation patterns still held with a smaller data set of calls, and how the effect of habitat compared to the effect of range (Table A9). The distributions of the three frequency modulation measurements were also visualized across range–habitat types (Fig. 4).

Effect sizes for habitat comparisons were calculated with respect to native agro-interface habitats, while effect sizes for range comparisons were calculated with respect to native range urban habitats. Therefore, for variables with positive values, Cliff's delta with a positive sign indicated larger overall values for any given acoustic measurement for either native range urban (compared to native range agro-interface calls) or invasive range urban calls (compared to native range urban calls). Likewise, negative values of Cliff's delta indicated larger overall values for any given acoustic measurement for either native range agro-interface calls or native range urban calls. The opposite was true for variables with negative values (e.g. peak–trough slope). Overall, our results suggested that both range and habitat influence acoustic structure of learned contact calls, likely through alterations of the social environment in invasive range and/or urban habitats compared to native range agro-interface habitats.

Robustness of Results to Inadvertent Repeated Sampling of Unmarked Individuals

As birds that were not intentionally repeatedly sampled were unmarked (see above, Recording contact calls), some calls in the large data set used for broad geographical resolution may represent repeated sampling of the same individuals. Such inadvertent repeated sampling of individuals was unlikely to influence the results presented here. First, the large data set that contained calls representing such repeated sampling of the same individuals was used to assess general structural differentiation with supervised machine learning approaches between ranges, not to assess unique individual signatures present in calls. Second, frequency

modulation patterns considered to contribute to individual signatures were compared between ranges using a reduced version of this large data set. In this analysis of frequency modulation patterns, 10 sites were randomly sampled per range and four calls were randomly sampled per site, reducing the likelihood that calls of repeatedly sampled individuals were included in these analyses. Third, individual identity content in individual signatures of contact calls was assessed using calls of known repeatedly sampled individuals only from the smaller data set used for this study (Table A5), in which calls had been assigned to a given marked or unmarked individual with high confidence.

Table A1

Map of analyses and measurements used to address research questions

Question	Main analyses	Measurements
Did invasion alter the social environment?	Compared proxies of local population sizes and maximum social group sizes between ranges	Estimates of total nests, nest densities and maximum flock sizes per range
How did invasion influence overall call structure and frequency modulation patterns?	Classified calls back to each range with supervised machine learning	Training and prediction performance of supervised random forests and stochastic gradient boosting models (1561 calls)
	Assessed the effect of range on specific acoustic measurements	Cliff's delta for 27 standard acoustic measurements and 3 customized frequency modulation measurements (80 calls)
	Assessed whether acoustic measurements with large effects of range also changed over 3 sampling years in the invasive range	Visualized distributions of 3 standard acoustic measurements and 3 frequency modulation measurements (115 calls)
How did invasion influence individual vocal signatures?	Obtained individual identity content in contact calls of repeatedly sampled individuals	Beecher's statistic calculated from Mel-frequency cepstral coefficients (50 calls) and frequency contours (50 calls)
How did habitat differences between ranges influence call structure?	Assessed the independent effects of habitat and range on specific acoustic measurements	Plots from principal components analysis, Cliff's delta for effect of habitat or range for 27 standard measurements (210 calls) and 3 frequency modulation measurements (24 calls)

Table A2

Nest estimates in the native and invasive ranges

Range	Year	Department or city, state	Site code	Estimated nests	Area (ha)	Nest density (nests/ ha)
Native	2017	Maldonado	PLVE	10	1.27	7.87
Native	2017	Colonia	RIAC	109	3.15	34.58
Native	2017	San José	ECIL	247	21.45	11.52
Native	2017	Colonia	INES-01	10	—	—
Native	2017	Colonia	SEMI	29	0.44	66.55
Native	2017	Colonia	INES-03	50	1.17	42.70
Native	2017	Colonia	INES-07	15	0.53	28.55
Native	2017	Colonia	INES-06	20	1.37	14.61
Native	2017	Colonia	INES-08	25	0.85	29.55
Native	2017	Colonia	INES-05	6	—	—
Native	2017	Colonia	1145	8	4.51	1.77
Native	2017	Colonia	ROSA	41	—	—
Native	2017	Colonia	CHAC	19	0.48	39.59
Native	2017	Canelones	INBR	20	0.77	25.86
Native	2017	Montevideo	BCAR	33	0.36	91.73
Native	2017	Maldonado	HIPE	15	0.38	39.85
Native	2017	Maldonado	QUEB	10	1.14	8.80
Native	2017	Maldonado	CISN	9	0.87	10.32
Native	2017	Colonia	PIED	38	0.77	49.19
Native	2017	Rocha	VALI	13	—	—
Invasive	2018	Gilbert, AZ	GILB	3	0.07	42.75
Invasive	2019	Austin, TX	INTR	13	1.05	12.32
Invasive	2019	Austin, TX	ELEM	1	—	—
Invasive	2019	Austin, TX	AIRP	5	0.28	17.73
Invasive	2019	Austin, TX	SOCC	12	2.13	5.64
Invasive	2019	Austin, TX	MANO	4	0.07	59.67
Invasive	2019	Austin, TX	MART	8	2.86	2.79
Invasive	2011	Austin, TX	MART	6	2.86	2.09
Invasive	2011	Austin, TX	VALL	2	—	—

Invasive	2011	Austin, TX	ELEM	4	—	—
Invasive	2011	Austin, TX	SOFT	6	0.64	9.30
Invasive	2011	Austin, TX	AIRP	2	—	—
Invasive	2011	Austin, TX	BART	1	—	—
Invasive	2011	Austin, TX	INTR	20	32.05	0.62
Invasive	2011	New Orleans, LA	ROBE	8	—	—
Invasive	2011	New Orleans, LA	LAKE	2	—	—
Invasive	2011	Dallas, TX	LAWT	4	0.22	17.95

Estimated numbers of nests, site areas and nest densities for a subset of recording sites, ordered from most recent to later sampling years per range. It was not possible to obtain site areas and nest densities for all sites shown here, as described in the main text. Full site names are shown in Table A3 and Table A4.

Table A3

Native range recording sites in Uruguay

	Site code	Site name	Department	Latitude	Longitude	N_{Calls}	Date
1	PIED	Piedra de los Indios	Colonia	-34.413	-57.849	21	25 Oct 2017
2	CHAC[1]	La Chacra de los Olivos	Colonia	-34.413	-57.843	12	21 Aug 2017
3	LENA	Las Leñas	Colonia	-34.411	-57.838	19	23 Oct 2017
4	PFER	Parque Ferrando	Colonia	-34.468,-34.465	-57.831, -57.827	53	19 Jun 2017, 21 Jun 201
5	INES-08	INIA La Estanzuela - 08	Colonia	-34.345	-57.733	27	13 Jul 2017
6	EMBR[1]	Embarcadero de Riachuelo	Colonia	-34.444	-57.728	23	17 Jul 2017, 21 Jul 2017
7	INES-01	INIA La Estanzuela - 01	Colonia	-34.349	-57.727	12	3 Jul 2017
8	INES-07	INIA La Estanzuela - 07	Colonia	-34.346	-57.710	9	13 Jul 2017
9	INES-06	INIA La Estanzuela - 06	Colonia	-34.344	-57.708	6	13 Jul 2017
10	RIAC	Riachuelo	Colonia	-34.436, -34.437	-57.706	25	28 Jun 2017
11	INES-05	INIA La Estanzuela - 05	Colonia	-34.340	-57.690	6	15 Jul 2017
12	SEMI	Semillero	Colonia	-34.326	-57.680	11	25 Jul 2017
13	INES-03	INIA La Estanzuela - 03	Colonia	-34.336	-57.668	15	11 Jul 2017
14	INES-04	INIA La Estanzuela - 04	Colonia	-34.335	-57.668	9	11 Jul 2017
15	ARAP	Las Termas del Arapey	Salto	-30.946	-57.520	12	7 May 2017
16	1145[1]	Ruta 1 km 145	Colonia	-34.375, -34.376	-57.502, -57.500	17	24 Jul 2017, 26 Jul 2017 28 Jul 2017, 29 Jul 2017
17	ROSA	Rosario	Colonia	-34.338	-57.336	15	27 Jul 2017
18	ECIL	Ecilda Paullier	San José	-34.360, -34.361	-57.060	17	28 Jul 2017
19	PAVO	Arroyo Pavón	San José	-34.442	-56.967	25	17 Oct 2017

20	ARAZ	Balneario de Arazati	San José	-34.535	-56.812	15	3 Nov 2017
21	KIYU	Balneario de Kiyú	San José	-34.607	-56.715	8	3 Nov 2017
22	BAGU	La Baguala	Montevideo	-34.848	-56.384	20	9 Oct 2017
23	INBR	INIA Las Brujas	Canelones	-34.668	-56.330	19	3 Sep 2017
24	PEIX	Camino Peixoto	Montevideo	-34.765	-56.279	19	6 Oct 2017
25	**BCAR**	**Bodegas Carrau**	Montevideo	-34.788	-56.223	13	20 Oct 2017
26	**FAGR**	**Facultad de Agronomía**	Montevideo	-34.838	-56.219	7	5 Sep 2017
27	**CEME**	**Cementerio Central**	Montevideo	-34.913	-56.187	6	18 Oct 2017
28	**GOLF**	**Club de Golf**	Montevideo	-34.923	-56.164	22	20 Nov 2017
29	PROO	Parque Roosevelt	Canelones	-34.855	-56.022	12	14 Sep 2017
30	PLVE	Plaza Venus, Piriápolis	Maldonado	-34.870	-55.264	11	21 May 2017
31	QUEB	Quebrada del Castillo	Maldonado	-34.834	-55.260	16	13 Sep 2017
32	CISN	La Laguna de los Cisnes	Maldonado	-34.861	-55.150	28	13 Sep 2017
33	SAUC	La Laguna del Sauce	Maldonado	-34.857	-55.041	6	12 Sep 2017
34	HIPE	Centro de Entrenamiento Hípico Punta del Este	Maldonado	-34.825	-55.010	5	12 Sep 2017
35	ELTE	El Tesoro	Maldonado	-34.889	-54.863	23	13 Sep 2017
36	VALI	Barra de Valizas	Rocha	-34.334	-53.803	23	16 Nov 2017
37	OJOS	Ojos de Agua	Rocha	-33.804	-53.506	23	16 Nov 2017

Native range recording sites and dates in Uruguay. Numbers of calls recorded per site are reported (610 total).

Recording sessions per site were typically performed in a single day. However, when assessing invasive range sites in Austin, Texas recorded in different years to harmonize site codes for temporal analyses (in which sites recorded relatively close to each other in different years were assigned the same site code), we also merged two pairs of native range sites that had been kept separate in previous analyses (PFER-01, PFER-03 and RIAC-01, RIAC-02) to represent very fine-scale geographical sampling (Smith-Vidaurre et al., 2020). RIAC-01 (8 calls) and RIAC-02 (17 calls) were recorded on the same day, but PFER-01 (19 calls) and PFER-03 (34 calls) recording sessions were from different days. Moreover, for an independent analysis, we added a single call per repeatedly sampled individual to the data set of a single call per unmarked individual per range, for consistency

with previous work. This preprocessing led to calls recorded on different days for sites EMBR and 1145 (see Appendix, Call selection in Raven and preprocessing calls in R for more details and Table A5 for repeatedly sampled individuals). The four urban sites at which we recorded calls are shown in bold.

[1] Sites at which we sampled marked or unmarked birds for the data set of repeatedly sampled individuals.

Table A4

Invasive range recording sites in the U.S.

	Site code	Site name	City, state	Latitude	Longitude	N_{Calls}	Date
1	GILB	Gilbert Town Square	Gilbert, AZ	33.331	-111.791	16	9 Apr 2018
2	LAWT	Lawther Substation	Dallas, TX	32.820	-96.730	9	20 Feb 2011
3	COMM	Austin Community College	Austin, TX	30.404	-97.705	11	30 Mar 2004
4	INTR	University of Texas (UT) – Austin Intramural fields	Austin, TX	30.316	-97.719	15	15 Feb 2011
5	INTR[1]	UT – Austin Intramural Fields	Austin, TX	30.317	-97.728	82	8 Aug 2019
6	MANO	Manor Rd.	Austin, TX	30.299	-97.686	5	9 Aug 2019
7	AIRP	Airport Boulevard	Austin, TX	30.285	-97.705	9	7 Aug 2019
8	SOFT	McCombs Softball Field	Austin, TX	30.281	-97.725	14	15 Feb 2011
9	SOCC	Soccer Field, César Chavez	Austin, TX	30.272	-97.767	77	30 Mar 2004
10	SOCC[1]	César Chavez Fields	Austin, TX	30.270	-97.761	93	9 Aug 2019
11	VALL	Pleasant Valley Rd.	Austin, TX	30.261	-97.711	5	30 Mar 2004
12	VALL	Pleasant Valley Rd. & 7th	Austin, TX	30.261	-97.711	10	15 Feb 2011
13	ELEM	UT Elementary School	Austin, TX	30.260	-97.718	12	15 Feb 2011
14	ELEM[1]	UT Elementary School	Austin, TX	30.260	-97.718	61	6 Aug 2019
15	MART	Sam L. Martin Middle School	Austin, TX	30.253	-97.731	14	15 Feb 2011
16	MART	Sam L. Martin Middle School	Austin, TX	30.251	-97.731	50	10 Aug 2019
17	LAKE	Lakeview Dr.	New Orleans, LA	30.029	-90.077	6	18 Feb 2011
18	FOLS	Folse Dr. & Harris St.	New Orleans, LA	30.027	-90.205	10	30 Mar 2004
19	ROBE[1]	Robert E. Lee Rd.	New Orleans, LA	30.021	-90.069	24	18 Feb 2011
20	BALL	Ballfield at corner of W. Esplanade & Oaklawn	New Orleans, LA	30.013	-90.132	26	30 Mar 2004
21	CANA	Canal Blvd.	New Orleans, LA	29.981	-90.110	13	30 Mar 2004

22	BAPT	Baptist Hospital	Miami, FL	25.688	-80.338	40	30 Mar 2004
23	BUCK	Buckingham Ave.	Milford, CT	41.217	-73.038	60	30 Mar 2004
24	MEAD	Meadowside Rd.	Milford, CT	41.210	-73.071	28	30 Mar 2004
25	SHAK	Shakespeare Theatre	Stratford, CT	41.184	-73.126	50	30 Mar 2004
26	AUDU	Milford Audubon	Milford, CT	41.176	-73.102	17	30 Mar 2004

Invasive range recording sites and dates in the U.S. Numbers of calls recorded per site are reported (757 total). Site details for calls recorded in 2004 were previously published (Buhrman-Deever et al., 2007). Specific recording dates were not provided with the 2004 call data set, so we assigned a single date to all 2004 sites within the dates reported by Buhrman-Deever et al. (2007). Geographical coordinates are also approximate for all 2004 sites, as we obtained these by entering site names in Google Maps. Site codes were harmonized over time for Austin, Texas, as described above (Table A2; also see Appendix, Call selection in Raven and preprocessing calls in R, for more details and Table A5 for repeatedly sampled individuals).

[1] Sites at which we repeatedly sampled unmarked individuals.

Table A5

Repeatedly sampled individuals per range

	Individual ID	Site code	Site name	Department or city, state	Latitude	Longitude	N_{Calls}	Date
1	NAT-AAT	1145	Ruta 1 km 145	Colonia	-34.376	-57.500	12	29 Jul 2017
2	NAT-UM1	1145	Ruta 1 km 145	Colonia	-34.375	-57.502	25	28 Jul 2017
3	NAT-UM2	1145	Ruta 1 km 145	Colonia	-34.375	-57.502	23	24 Jul 2017
4	NAT-UM3	1145	Ruta 1 km 145	Colonia	-34.375	-57.502	5	24 Jul 2017
5	NAT-UM4	1145	Ruta 1 km 145	Colonia	-34.376	-57.500	13	26 Jul 2017
6	NAT-UM5	CHAC	La Chacra de los Olivos	Colonia	-34.413	-57.843	7	21 Aug 2017
7	NAT-RAW	EMBR	Embarcadero de Riachuelo	Colonia	-34.444	-57.728	4	17 Jul 2017
8	NAT-ZW8	EMBR	Embarcadero de Riachuelo	Colonia	-34.444	-57.728	8	21 Jul 2017
9	INV-UM6	ASCA	Ascarate Park	El Paso, TX	31.754	-106.405	25	10 Mar 2019
10	INV-UM10	INTR	University of Texas (UT) – Austin Intramural fields	Austin, TX	30.317	-97.728	6	8 Aug 2019
11	INV-UM7	ELEM	UT Elementary School	Austin, TX	30.260	-97.718	28	6 Aug 2019
12	INV-UM9	ELEM	UT Elementary School	Austin, TX	30.260	-97.718	5	6 Aug 2019
13	INV-UM16	SOCC	César Chavez Fields	Austin, TX	30.270	-97.761	8	9 Aug 2019
14	INV-UM17	SOCC	César Chavez Fields	Austin, TX	30.270	-97.761	5	9 Aug 2019
15	INV-UM1	BART	Bartholomew Park	Austin, TX	30.305	-97.695	23	15 Feb 2011
16	INV-UM5	ROBE	Robert E. Lee Rd	New Orleans, LA	30.021	-90.069	20	18 Feb 2011
17	INV-UM19	CAME	Robert E. Lee & Cameron Rd	New Orleans, LA	30.022	-90.065	12	30 Mar 2004

Number of calls, recording locations and dates for known repeatedly sampled individuals per range (229 total calls). Each individual was recorded on a single day. Native range individuals (prefix ‘NAT’ in the individual ID column) were recorded in Uruguay in 2017, while invasive individuals (prefix ‘INV’ in the individual ID

column) were recorded in the U.S in 2019, 2011 or 2004. Site CAME in 2004 was close to the site labelled ROBE recorded in 2011, but we did not harmonize site codes to be the same over time for the data set of repeatedly sampled individuals. The recording date for individual INV-UM19 at CAME 2004 is an approximate date from previously published work (Buhrman-Deever et al., 2007).

Table A6

Supervised machine learning performance metrics

Model	Training accuracy (%) and 95% CI	Final parameters	Validation accuracy (%)	Prediction accuracy (%)
Stochastic gradient boosting	92.28 (91.33, 93.16)	n.trees = 1600, interaction.depth = 3, shrinkage = 0.1, nminobsinnode = 1	—	—
Random forests	91.09 (90.08, 92.03)	mtry = 2, splitrule = gini, min.node.size = 1, n.trees = 2000	91.99	87.59

Supervised machine learning models classified calls back to the correct range with high accuracy, pointing to overall differences in call structure between ranges. Models were trained to classify calls back to the native or invasive range. The random forests model was selected for validation and prediction as described in the text.

Table A7

Effect sizes of range with 95% CI for 18 acoustic measurements

	Measurement	Native range median (IQR)	Invasive range median (IQR)	Effect size: Cliff's delta (95% CI)
1	Standard deviation of frequency	1.692 (0.161)	1.864 (0.191)	**0.78 (0.61, 0.89)**
2	Number of peaks	6.000 (1.000)	4.500 (1.000)	**-0.69, (-0.82, -0.49)**
3	Peak–trough slope	-0.411 (0.136)	-0.309 (0.063)	**0.69 (0.48, 0.83)**
4	Modulation rate	32.833 (4.891)	26.334 (8.826)	**-0.63 (-0.79, -0.41)**
5	Spectral flatness	0.583 (0.077)	0.631 (0.082)	**0.58 (0.35, 0.75)**
6	Entropy	0.834 (0.009)	0.841 (0.015)	**0.51 (0.27, 0.69)**
7	Spectral entropy	0.938 (0.016)	0.943 (0.015)	*0.45 (0.20, 0.64)*
8	Frequency interquartile range	2.026 (0.292)	2.377 (0.638)	*0.44 (0.19, 0.64)*
9	Third quartile time	0.121 (0.018)	0.112 (0.013)	*-0.34 (-0.56, -0.08)*
10	Dominant frequency range	4.025 (1.750)	4.492 (0.846)	*0.32 (0.06, 0.55)*
11	Mean peak frequency	4.083 (0.467)	3.383 (1.225)	*-0.32 (-0.56, -0.07)*
12	Duration	0.171 (0.013)	0.165 (0.024)	*-0.29 (-0.52, -0.03)*
13	Time entropy	0.889 (0.002)	0.890 (0.005)	*0.29 (0.02, 0.52)*
14	Time interquartile range	0.075 (0.013)	0.070 (0.011)	*-0.28 (-0.52, -0.02)*
15	Modulation index	10.339 (4.803)	9.039 (3.485)	*-0.27 (-0.50, -0.01)*
16	First quartile frequency	2.914 (0.483)	2.754 (0.500)	-0.26 (-0.50, 0.01)
17	Maximum dominant frequency	4.958 (0.379)	5.133 (1.079)	0.26 (0, 0.49)
18	End dominant frequency	3.033 (2.625)	1.225 (2.158)	-0.26 (-0.50, 0)
19	Median time	0.082 (0.012)	0.078 (0.011)	-0.25 (-0.49, 0)
20	First quartile time	0.046 (0.010)	0.044 (0.006)	-0.24 (-0.47, 0.02)
21	Peak frequency	3.122 (1.370)	2.871 (0.859)	-0.24 (-0.48, 0.02)
22	Mean dominant frequency	3.479 (0.361)	3.352 (0.448)	-0.22 (-0.46, 0.04)
23	Median frequency	3.961 (0.408)	3.859 (0.469)	-0.19 (-0.43, 0.08)
24	Third quartile frequency	4.962 (0.643)	5.059 (0.665)	0.19 (-0.07, 0.43)
25	Start dominant frequency	2.217 (2.275)	0.992 (1.575)	-0.17 (-0.41, 0.09)
26	Kurtosis	8.009 (2.276)	8.364 (3.673)	0.16 (-0.1, 0.41)
27	Minimum dominant frequency	0.758 (1.429)	0.642 (0.350)	-0.16 (-0.39, 0.1)
28	Skew	2.071 (0.342)	2.054 (0.490)	0.07 (-0.19, 0.32)
29	Mean frequency	4.048 (0.413)	4.044 (0.482)	-0.06 (-0.32, 0.20)

30	Dominant frequency slope	2.003 (19.876)	1.356 (5.679)	-0.04 (-0.29, 0.23)

Summary statistics and the effect of range are presented for 30 different acoustic measurements, in which each range was represented by 40 calls (80 calls total). Shown are the medians, interquartile ranges (IQR) and effect sizes of range (Cliff's delta and bootstrapped 95% confidence intervals, CIs) in order of decreasing absolute effect size (top to bottom). Medians and IQRs are shown with three decimal points to emphasize differences in acoustic measurements with smaller values (spectral entropy). Frequency measurements are in kHz and temporal measurements are displayed in seconds, while modulation rate is in peaks/second. Peak–trough slope represents change in kHz/change in indices of spline-interpolated points. Large and statistically significant effect sizes (with 95% CIs that did not include 0) are in bold, and smaller but still statistically significant effect sizes are shown in italics. Negative effect sizes indicate higher measurement values for the native range, with the exception of peak–trough slope (for which the absolute measurements were higher for the native range).

Table A8

Effect sizes of habitat and range on standard acoustic parameters

Comparison	Measurement	Effect size: Cliff's delta (95% CI)
Habitat	Duration	**-0.66 (-0.79, -0.47)**
	Time entropy	**0.66 (0.47, 0.80)**
	Third quartile time	**-0.64 (-0.78, -0.45)**
	Time interquartile range	**-0.60 (-0.75, -0.41)**
	Median time	**-0.48 (-0.64, -0.28)**
	First quartile time	-0.44 (-0.61, -0.25)
	Modulation index	-0.31 (-0.49, -0.12)
	Entropy	0.30 (0.09, 0.49)
	First quartile frequency	-0.29 (-0.48, -0.09)
	Frequency interquartile range	0.21 (0.01, 0.41)
Range	Standard deviation of frequency	**0.60 (0.43, 0.73)**
	Dominant frequency range	**0.57 (0.37, 0.72)**
	Minimum dominant frequency	**-0.55 (-0.70, -0.38)**
	End dominant frequency	**-0.51 (-0.68, -0.29)**
	Spectral entropy	**0.48 (0.28, 0.63)**
	Spectral flatness	0.45 (0.26, 0.61)
	Entropy	0.40 (0.20, 0.57)
	Start dominant frequency	-0.34 (-0.52, -0.13)
	Frequency interquartile range	0.32 (0.12, 0.50)
	Maximum dominant frequency	0.31 (0.10, 0.48)
	Time entropy	-0.26 (-0.45, -0.04)
	Duration	0.25 (0.03, 0.44)

Here, the habitat comparison represents native range urban calls compared to native range agro-interface calls, while invasive range urban calls were compared to native range urban calls to assess the effect of range. Effect sizes are shown as Cliff's delta with bootstrapped 95% confidence intervals (CIs) in decreasing order by absolute magnitude per comparison. Only acoustic measurements with significant effects of habitat or range are shown (e.g. measurements that displayed effect sizes with 95% CIs that did not include zero). Large effect sizes are bolded, following a rule-of-thumb described above.

Table A9

Frequency modulation patterns by range and habitat

Comparison	Measurement	Effect size and 95% CI
Habitat	Number of peaks	**-0.77 (-0.92, -0.16)**
	Modulation rate	**-0.62 (-1.00, -0.06)**
	Peak–trough slope	-0.25 (-0.75, 0.34)
Range	Peak–trough slope	**0.91 (0.25, 1.00)**
	Number of peaks	**-0.66 (-0.92, -0.16)**
	Modulation rate	-0.56 (-0.91, 0)

The habitat and range comparisons were performed as in Table A8, although with a smaller set of sites and calls per range and habitat (see Appendix, Validating the Effect of Urban and Agro-interface Habitats between Ranges). Effect sizes are shown as Cliff's delta with bootstrapped 95% confidence intervals (CIs) in decreasing order by absolute magnitude per comparison. Large and statistically significant effect sizes are bolded, following a rule-of-thumb described above.

Table 1

Beecher's statistic and possible unique individual signatures

Acoustic measurements	Range	N_{Calls}	HS	$N_{Signatures}$
MFCC	Native	25	2.77	7.67
	Invasive	25	2.37	5.62
Second harmonic	Native	25	2.05	4.20
	Invasive	25	1.09	1.19

Individual identity content in calls of repeatedly sampled individuals per range, using Beecher's information statistic (HS) with two measurements: descriptive statistics of Mel-frequency cepstral coefficients (MFCC) and second harmonic frequency contours. $N_{Signatures}$ is the number of possible unique individual signatures predicted by HS, and five calls for each of five individuals were used per calculation per range.

Figure 1. The estimated number of total nests, nest site area, nest density and maximum estimated flock sizes in the native (dark blue symbols) and invasive (gold symbols) ranges. Each panel displays the distribution of each variable per range with a box plot and raincloud plot. Box plots display the median, hinges (first and third quartiles) and whiskers (no further than 1.5 times the interquartile range beyond each hinge) of the data distribution per variable. Raincloud plots display the raw data points ('rain') and probability distribution ('cloud') per variable (Allen, Poggiali, Whitaker, Marshall, & Kievit, 2019). Asterisks mark variables that were statistically significantly different between ranges using two-sided Mann–Whitney–Wilcoxon tests.

Figure 2. Contact call structure for each range. (a) An example lexicon is shown with spectrograms of three randomly selected calls from three sites per range, in which each call represents a unique individual. The calls shown were sampled over similar geographical areas per range. Native (blue shading) and invasive (gold shading) range calls shown were recorded in 2017 and 2019, respectively. (b) Estimated kernel density contours are displayed in random forests acoustic space for the prediction data set. Contours delineate bins of density values coloured by range (native = blue lines; invasive = gold lines), with each bin representing 1/10th of the total density per range. Dimension 1 coordinates were flipped to place native range contours on the left-hand side. Here, the areas of the greatest densities of calls per range (contours of smaller areas that are also closer together) occupy distinct parts of acoustic space, pointing to structural differences in calls between ranges.

Figure 3. Frequency modulation patterns of calls recorded in the native (blue symbols) and invasive (gold symbols) ranges. (a) Examples of spline-smoothed second harmonic frequency contours with estimated peaks and troughs (red Xs and inverted turquoise triangles, respectively). Each call was randomly selected from a different site per range. Spline interpolation was applied to 90 manually traced points to obtain smoothed contours of over 400 points. (b) Data distributions of acoustic measurements with the largest effects of range, in decreasing order of absolute effect size magnitude (left to right). Each panel displays a box plot and raincloud plot per range, as in Fig. 1. Spectral flatness is an acoustic measurement similar to entropy, such that higher

values closer to 1 indicate noisier and less ordered acoustic signals (Araya-Salas et al., 2017). (c) Beecher's statistic and the number of possible unique individual signatures calculated using frequency contours and Mel-frequency cepstral coefficients.

Figure 4. Frequency modulation patterns of native and invasive range urban calls compared to native range agro-interface calls. Data distributions are shown for each of the three customized frequency modulation measurements. Each panel displays a box plot and raincloud plot per range–habitat, as in Fig. 1. Range–habitats are encoded with distinct colours (native range agro-interface = dark blue; native range urban = skyblue; invasive range urban = gold). Twenty-four calls total are shown here (8 calls from 2 sites each per range–habitat; see Appendix, Effects of habitat and range on acoustic measurements).

Figure A1. Frequency modulation patterns for invasive range calls (blue symbols) over 15 years of sampling and for 40 native range calls (gold symbols) recorded in 2017 that were used for the comparison between ranges. Data distributions are shown for the same acoustic measurements that displayed significant effects of range in Fig. 3b. Each panel displays a box plot and raincloud plot per range-year, similar to Fig. 1. Forty native range calls recorded in 2017 that were used for the comparison between ranges are shown for comparison. Each call used here represented a unique individual and was subsampled from the large data set of calls with broad geographical resolution.

Figure A2. Validation of repeatedly sampled individuals used for Beecher's statistic calculations. Shown are the mean differences in dynamic time warping (DTW) distance of second harmonic frequency contours within an individual compared to among individuals at either a single site (native range only) or three sites (both ranges). The single site comparison is missing for the invasive range due to insufficient sampling of individuals. Five individuals were used per comparison. The 95% confidence intervals (CIs) were generated by resampling with 1000 iterations. These results suggested that using three geographically proximate sites in the invasive range

provided patterns of variation among individuals equivalent to using a single site in the native range, and supported using these invasive range individuals for direct comparisons of Beecher's statistic between ranges. The native range results are shown in dark blue, and invasive range results are displayed in gold.

Figure A3. Urban calls in each range occupied a more similar area in acoustic space compared to native range agro-interface calls. Acoustic space was generated using principal components analysis with 27 spectral acoustic measurements. Density in acoustic space is represented with density contours colored by range–habitat, and each contour represents a bin of 1/10th of the density per range–habitat. Central contours are the smallest and innermost contours shown per range–habitat. Central contours for the native range urban and invasive range urban calls were closer together in acoustic space compared to the central contour for native range agro-interface calls. Range–habitats are encoded with distinct colors (native range agro-interface in dark blue, native range urban in sky blue, and invasive range urban in gold).

Figure 1

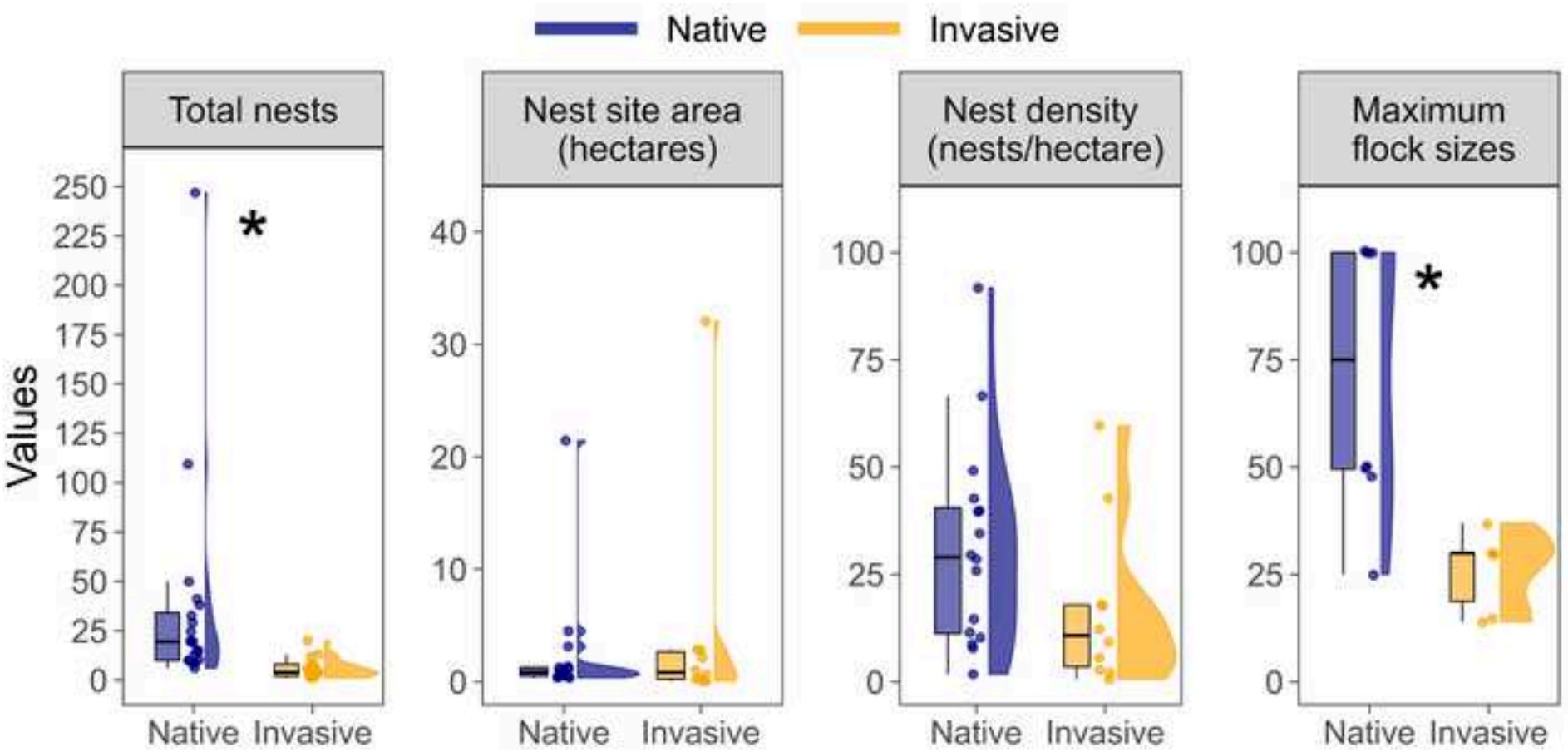

Figure 2 rev

Click here to access/download;Figure;Fig2_REV.jpeg

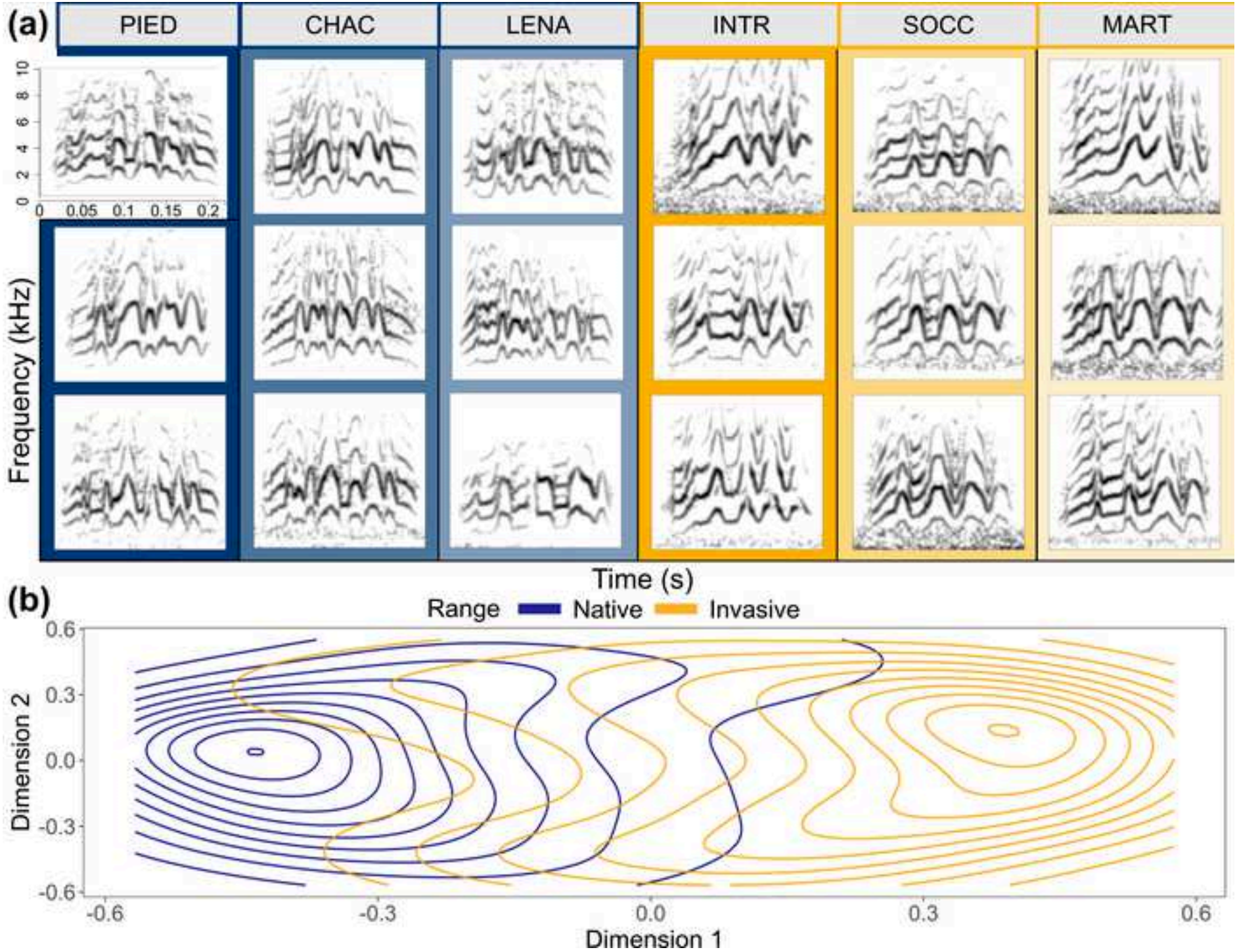

Figure 3 rev

Click here to access/download;Figure;Fig3_REV.jpeg

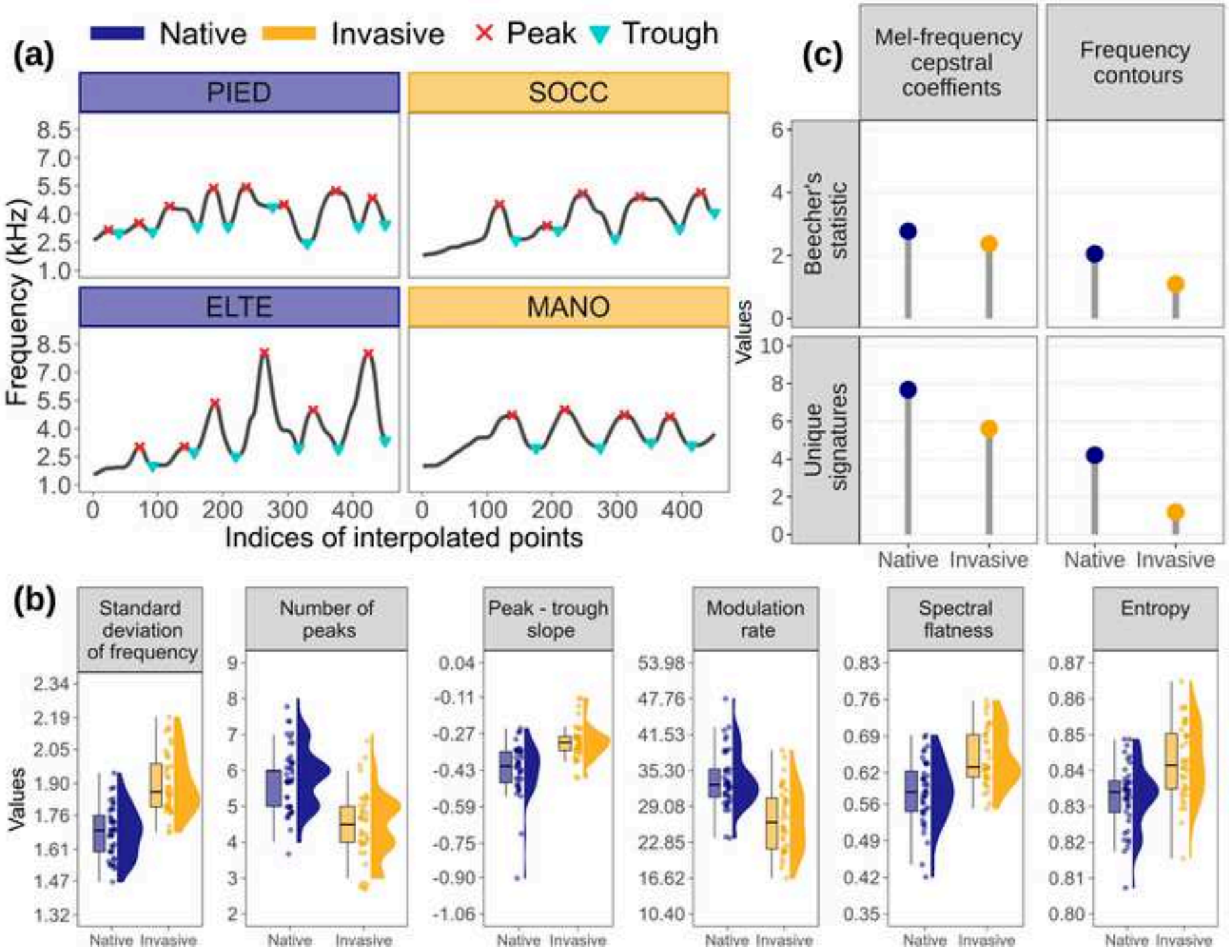

Figure 4

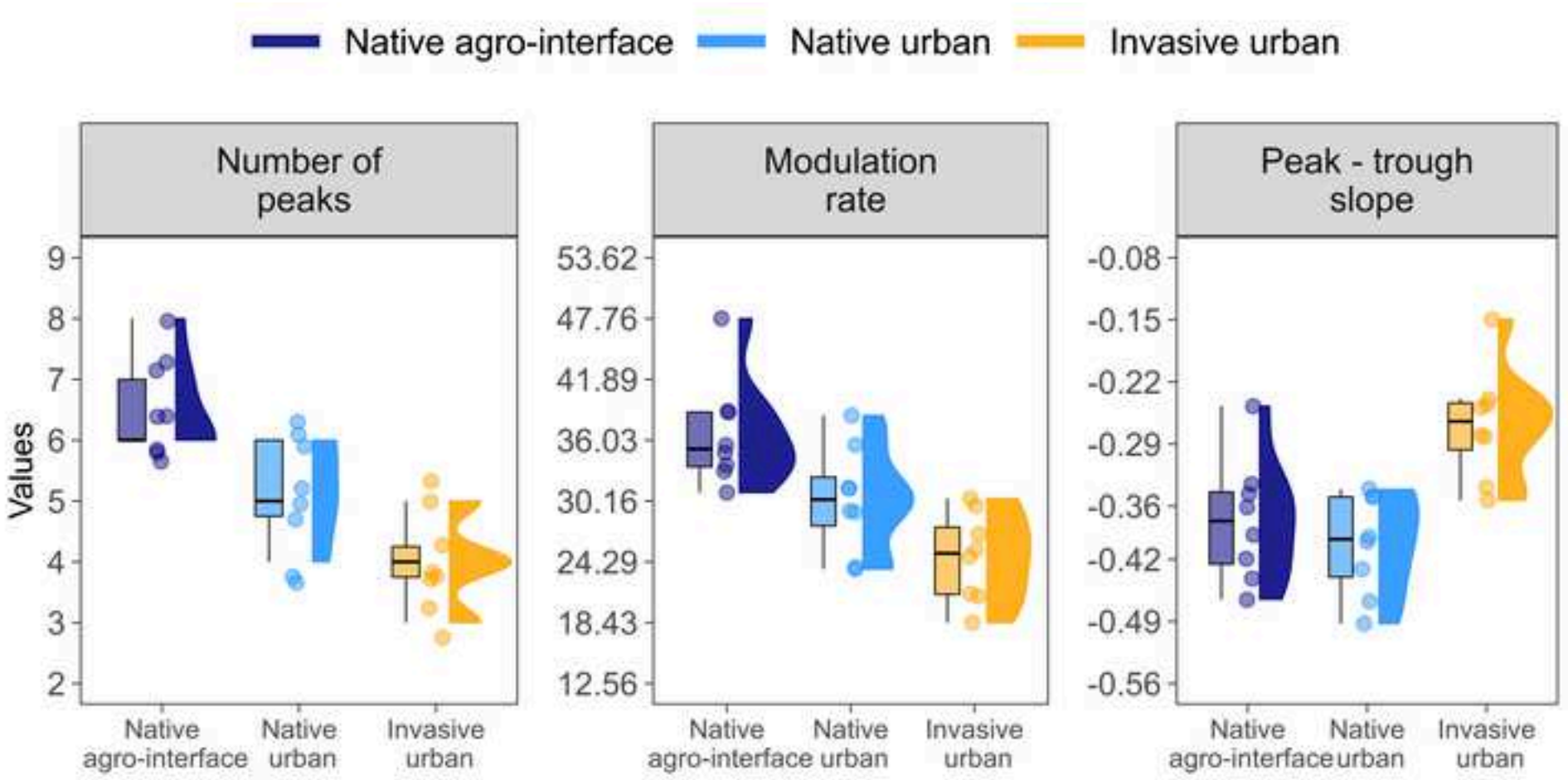

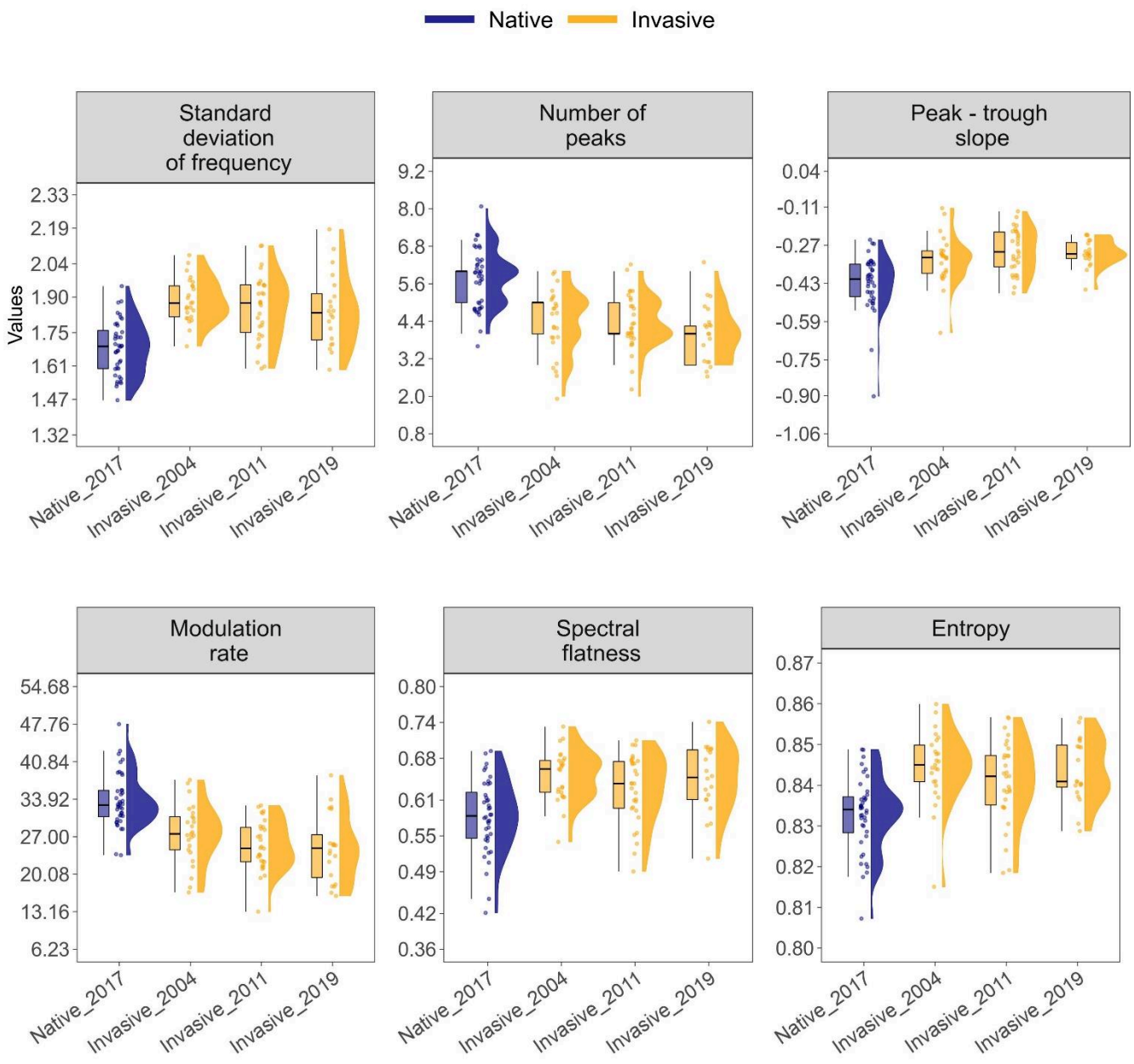

Fig. A1

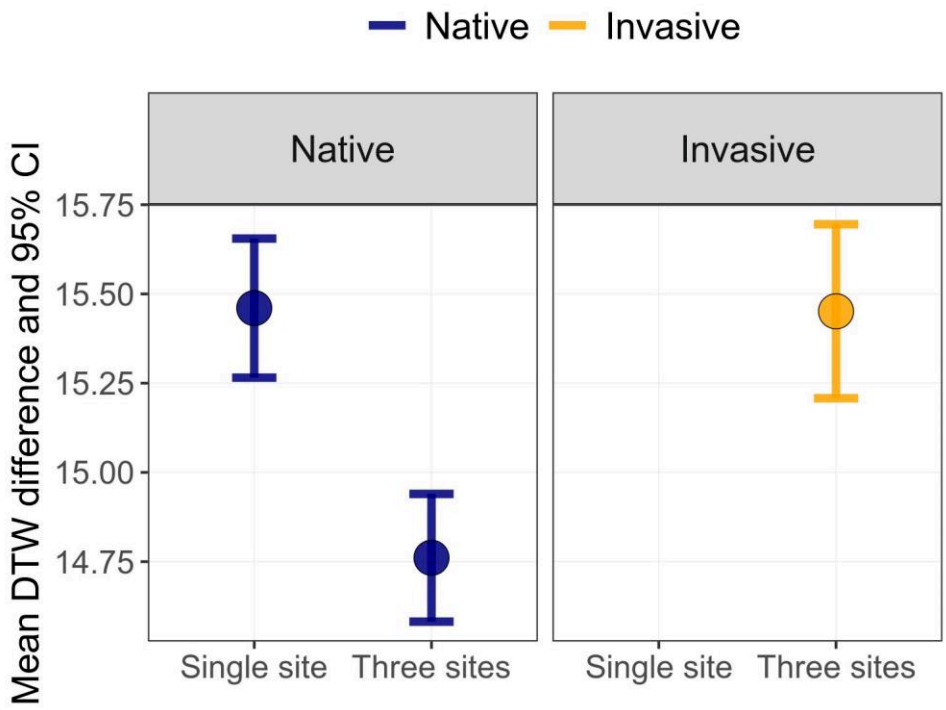
Native
Invasive
Native
Invasive
Mean DTW difference and 95% CI
15.75
15.50
15.25
15.00
14.75
Single site
Three sites
Single site
Three sites

Fig. A2

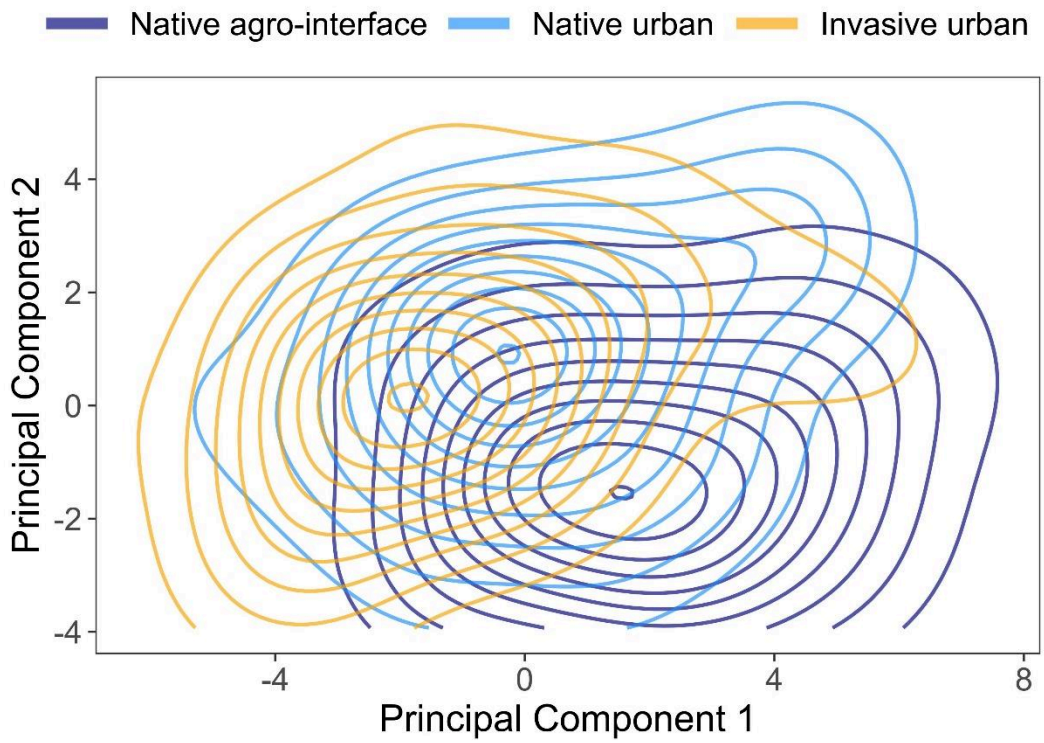
Native agro-interface
Native urban
Invasive urban
Principal Component 2
4
2
0
-2
-4
-4
0
4
8
Principal Component 1

Fig. A3